

Frustrations, memory, and complexity in classical and quantum spin systems

Mikhail Katsnelson

Main collaborators

**Andrey Bagrov, Tom Westerhout, Askar Iliasov, Alex Kolmus,
Bert Kappen, Alex Khajetoorians, Daniel Wegner and others,
Radboud University**

**Olle Eriksson, Anders Bergman, Diana Iuşan and others,
Uppsala University**

Vladimir Mazurenko and Ilia Iakovlev, Ural Federal University

Alessandro Principi, Manchester University

Epigraph with explanations

All science is either physics of stamp collection (E. Rutherford)



In stamp collection we deal with **history** and **complexity**

But the same in biology, geology... To understand the origin of cats and mice we need to go billions years to the past

Fundamental physical laws are **local** in time and space

What are the physical mechanisms of “stamp collection”?!

Outline

Introduction

Pattern formation in physics: magnetic patterns as an example

Structural complexity from magnetic patterns to art objects

Self-induced glassiness and beyond: the role of frustration

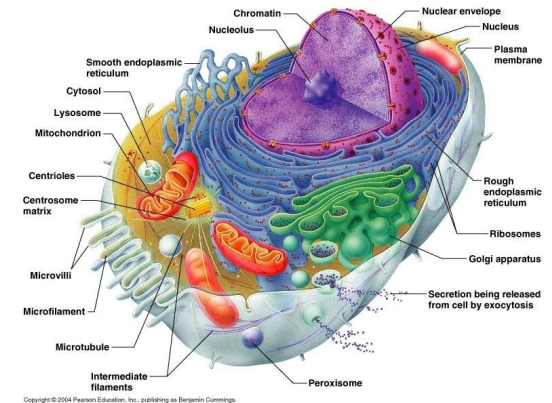
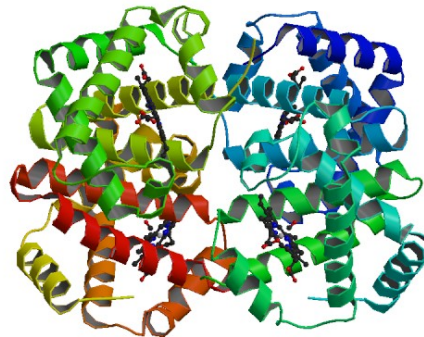
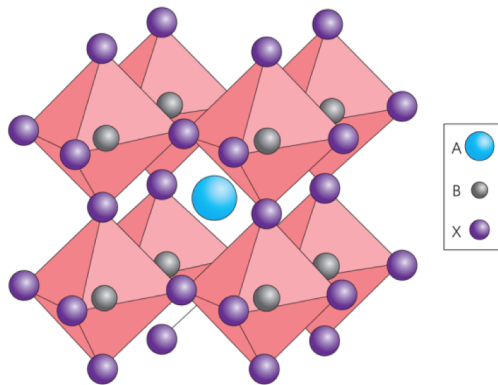
Experimental realization: elemental Nd

Complexity of quantum frustrated systems

Complexity

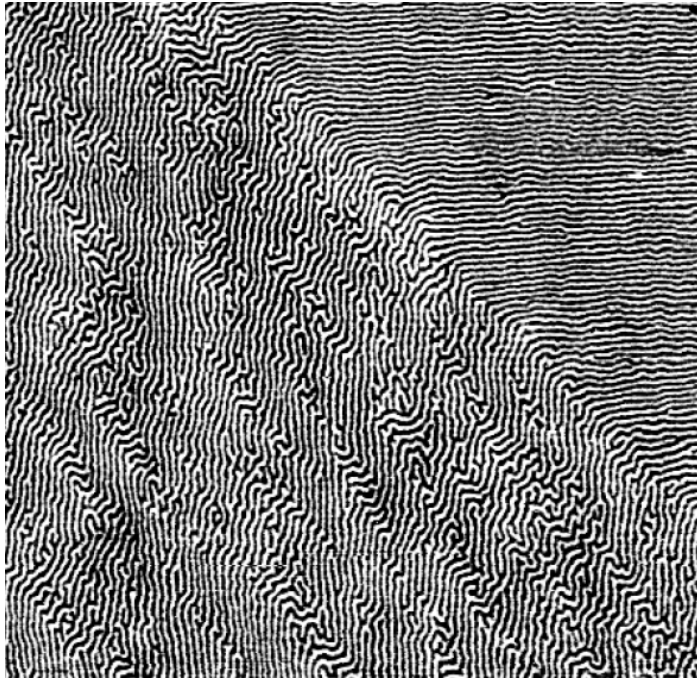
Schrödinger: life substance is “aperiodic crystal” (modern formulation – Laughlin, Pines and others – glass)

Intuitive feeling: crystals are simple, biological structures are complex



Origin and evolution of life: origin of complexity?

Complexity (“patterns”) in inorganic world

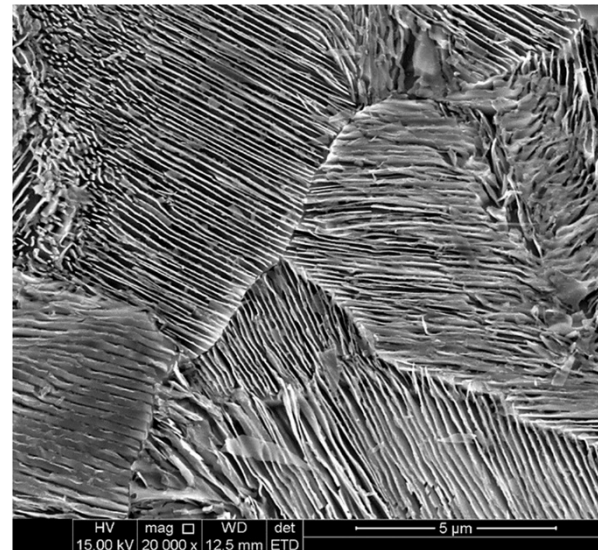


Stripe domains in ferromagnetic thin films



Stripes on a beach in tide zone

Microstructures in metals
and alloys



Pearlitic structure
in rail steel
(Sci Rep 9,
7454 (2019))

Do we understand this? No, or, at least, not completely

Magnetic patterns

Example: strip domains in thin ferromagnetic films

PHYSICAL REVIEW B 69, 064411 (2004)

Magnetization and domain structure of bcc $\text{Fe}_{81}\text{Ni}_{19}/\text{Co}$ (001) superlattices

R. Bručas, H. Hafermann, M. I. Katsnelson, I. L. Soroka, O. Eriksson, and B. Hjörvarsson

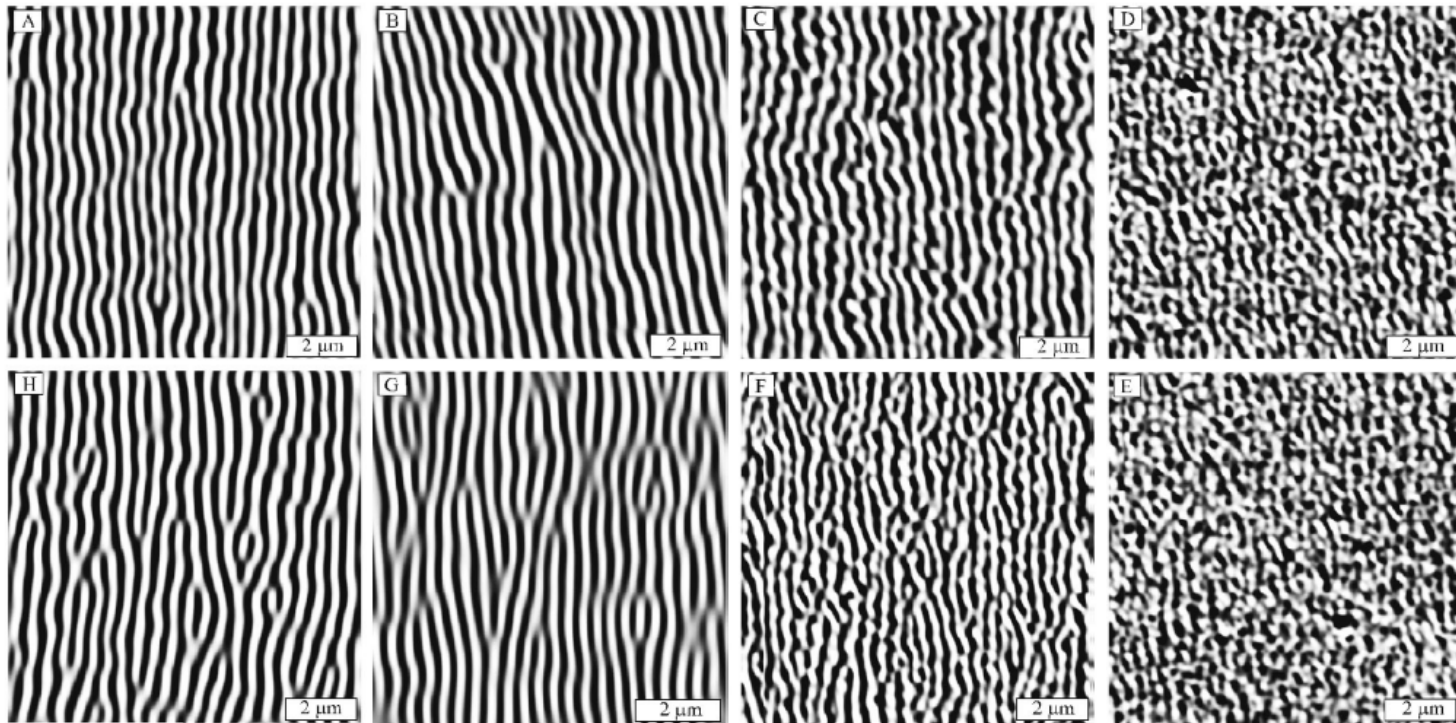
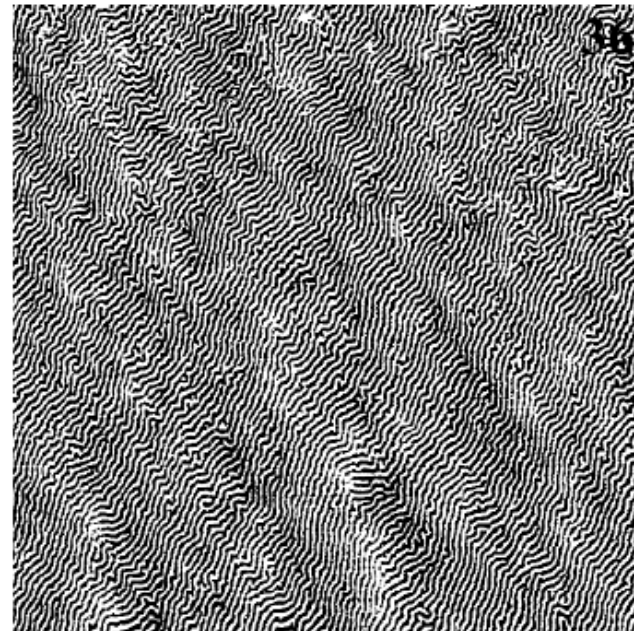
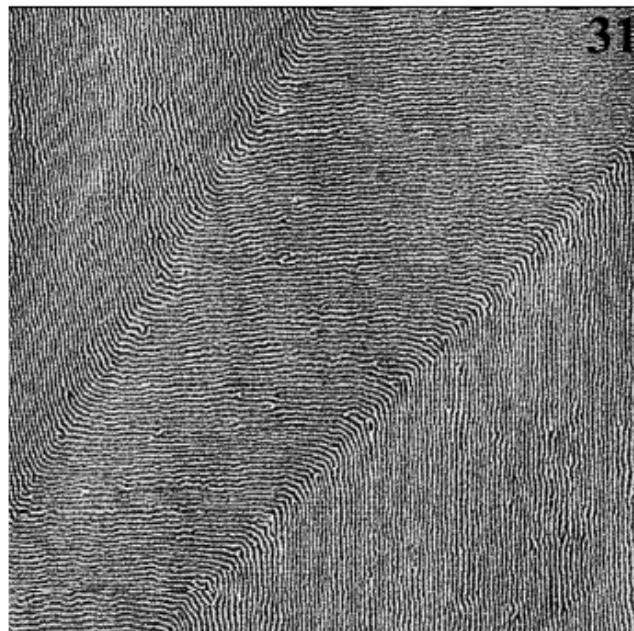
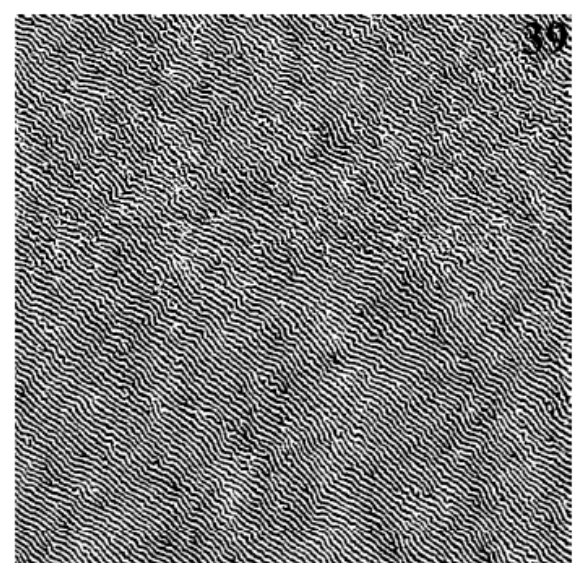
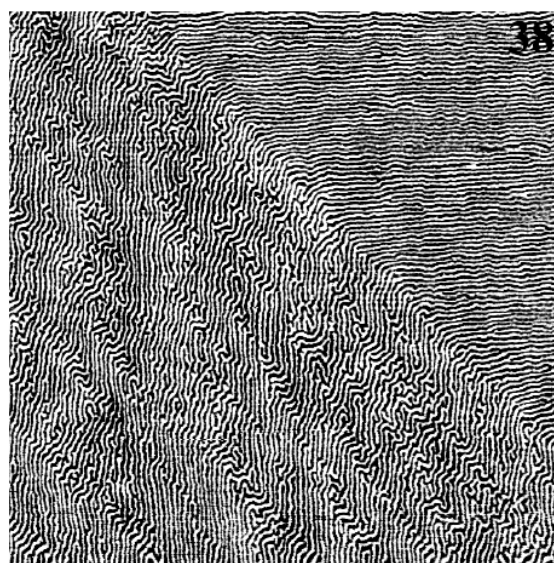
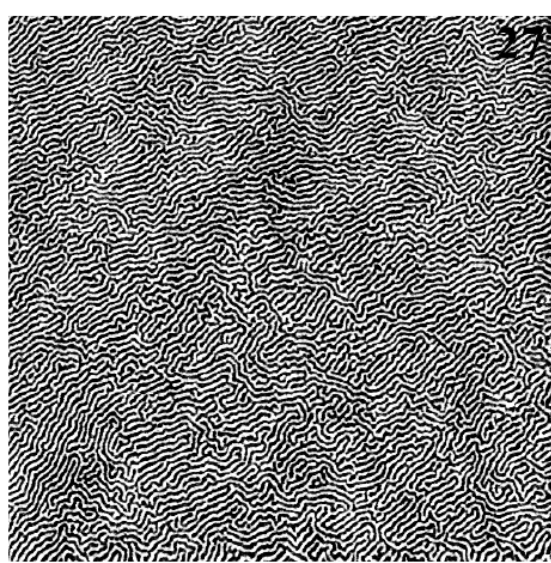


FIG. 2. The MFM images of the 420 nm thick $\text{Fe}_{81}\text{Ni}_{19}/\text{Co}$ superlattice at different externally applied in-plane magnetic fields: (a)—virgin (nonmagnetized) state; (b), (c), (d)—increasing field 8.3, 30, and 50 mT; (e), (f), (g)—decreasing field 50, 30, 8.3 mT; (h)—in remanent state.

Magnetic patterns II



Magnetic patterns III

Europhys. Lett., **73** (1), pp. 104–109 (2006)

DOI: 10.1209/epl/i2005-10367-8

Topological defects, pattern evolution, and hysteresis
in thin magnetic films

P. A. PRUDKOVSKII¹, A. N. RUBTSOV¹ and M. I. KATSNELSON²

$$H = \int \left(\frac{J_x}{2} \left(\frac{\partial \mathbf{m}}{\partial x} \right)^2 + \frac{J_y}{2} \left(\frac{\partial \mathbf{m}}{\partial y} \right)^2 - \frac{K}{2} m_z^2 - h m_y \right) d^2 r + \\ + \frac{Q^2}{2} \int \int m_z(\mathbf{r}) \left(\frac{1}{|\mathbf{r} - \mathbf{r}'|} - \frac{1}{\sqrt{d^2 + (\mathbf{r} - \mathbf{r}')^2}} \right) m_z(\mathbf{r}') d^2 r d^2 r'.$$

Competition of exchange interactions (want homogeneous ferromagnetic state) and magnetic dipole-dipole interactions (want total magnetization equal to zero)

Magnetic patterns IV

Classical Monte Carlo simulations

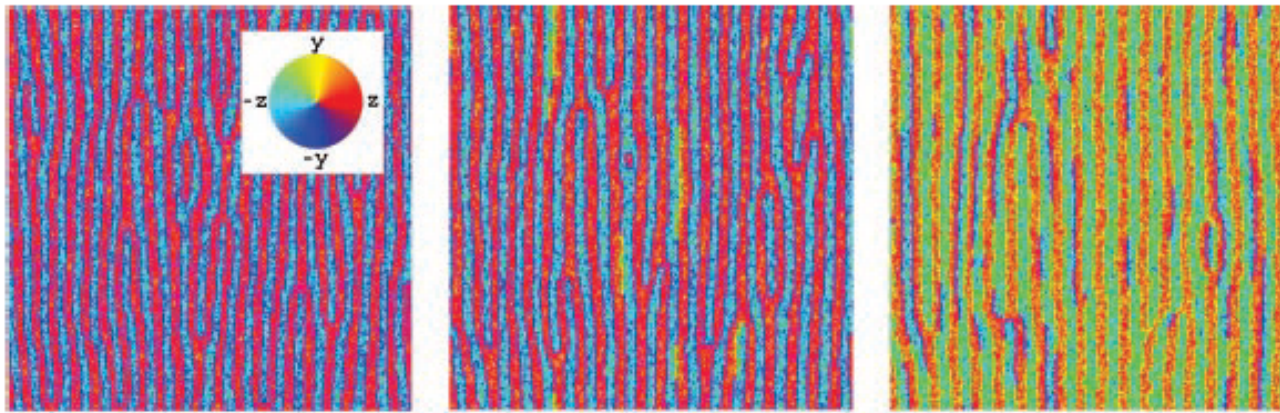


Fig. 2 – Snapshots of the stripe-domain system with the two-component order parameter at several points of the hysteresis loop for $\beta = 1$. The magnetic field is $h = 0$, $h = 0.3$, and $h = 0.6$, from left to right. The inset shows the color legend for the orientation of local magnetization.

We know the Hamiltonian and it is not very complicated

How to **describe** patterns and how to **explain** patterns?

What is complexity?

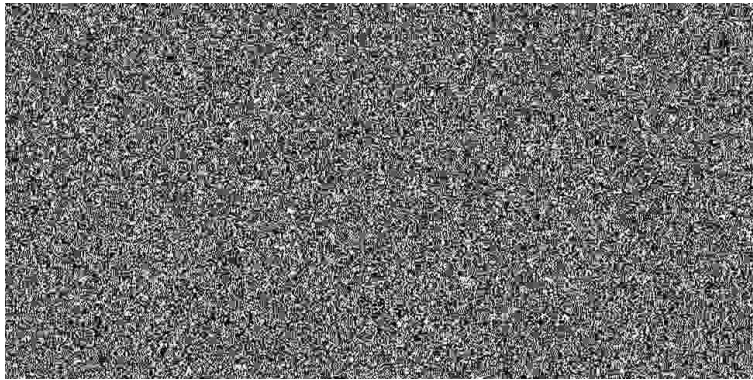
- Something that we immediately recognize when we see it, but very hard to define quantitatively
- S. Lloyd, “Measures of complexity: a non-exhaustive list” – 40 different definitions
- Can be roughly divided into two categories:
 - computational/descriptive complexities (“ultraviolet”)
 - effective/physical complexities (“infrared” or inter-scale)

Computational and descriptive complexities

- Prototype – the Kolmogorov complexity:
the length of the shortest description (in a given language) of the object of interest
- Examples:
 - Number of gates (in a predetermined basis) needed to create a given state from a reference one
 - Length of an instruction required by file compressing program to restore image

Descriptive complexity

- The more random – the more complex:



White noise

970 x 485 pixels, gray scale, 253 Kb

>



Vermeer “View of Delft”

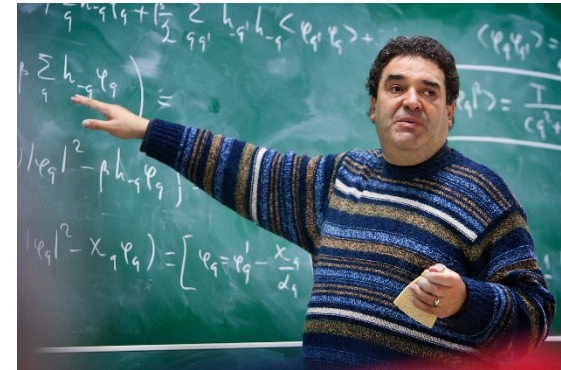
750 x 624 pixels, colored, 234 Kb

Descriptive complexity

- The more random – the more complex:

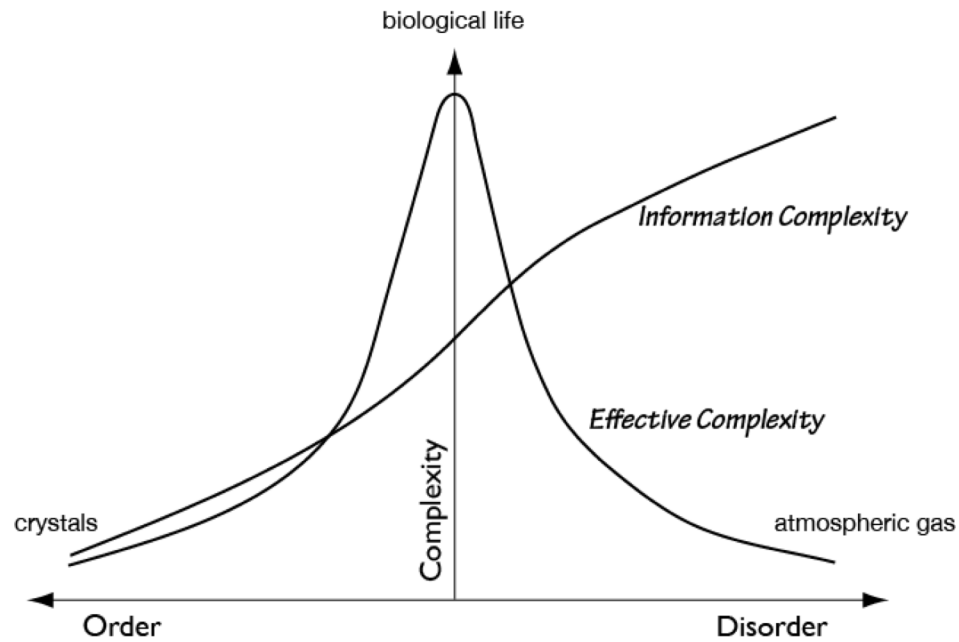


Paris japonica - 150
billion base pairs in
DNA



Homo sapiens - 3.1
billion base pairs in
DNA

Effective complexity



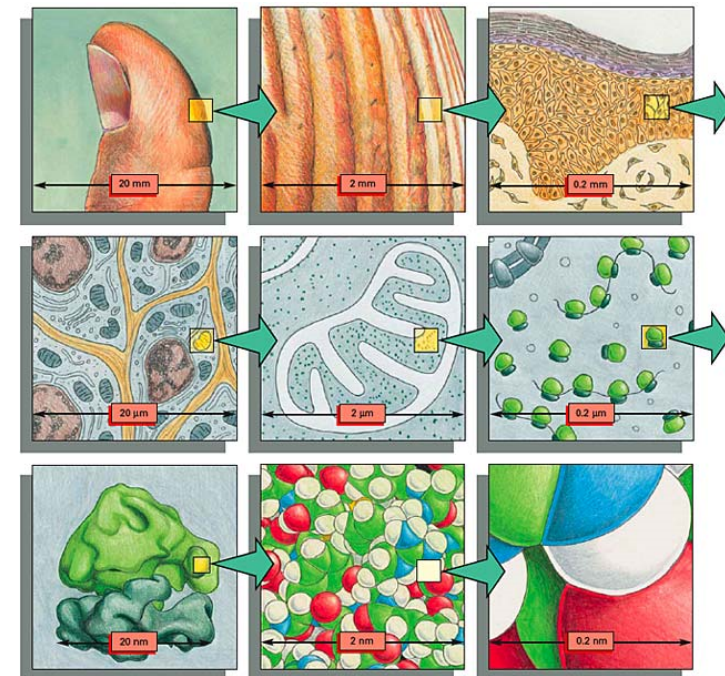
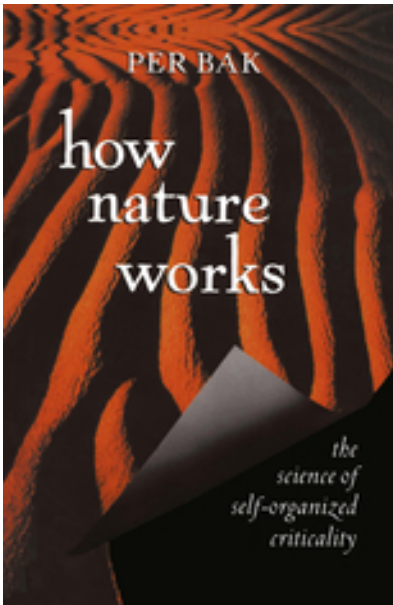
Can we come up with a quantitative measure?..

Attempts: Self-Organized Criticality

Per Bak: Complexity *is* criticality

Some complicated (marginally stable) systems demonstrate self-similarity and “fractal” structure

This is intuitively more complex behavior than just white noise but can we call it “complexity”?



I am not sure – **complexity is hierarchical**

Structural complexity

Multi-scale structural complexity of natural patterns

PNAS 117, 30241 (2020)

Andrey A. Bagrov^{a,b,1,2}, Ilia A. Iakovlev^{b,1}, Askar A. Iliasov^c, Mikhail I. Katsnelson^{c,b}, and Vladimir V. Mazurenko^b

The idea (from holographic complexity and common sense):
Complexity is **dissimilarity** at various scales

Let $f(x)$ be a multidimensional pattern

$f_\Lambda(x)$ its coarse-grained version (Kadanoff decimation, convolution with Gaussian window functions,...)

Complexity is related to distances between $f_\Lambda(x)$ and $f_{\Lambda+d\Lambda}(x)$

$$\Delta_\Lambda = |\langle f_\Lambda(x) | f_{\Lambda+d\Lambda}(x) \rangle -$$

$$\frac{1}{2} (\langle f_\Lambda(x) | f_\Lambda(x) \rangle + \langle f_{\Lambda+d\Lambda}(x) | f_{\Lambda+d\Lambda}(x) \rangle) =$$

$$\frac{1}{2} |\langle f_{\Lambda+d\Lambda}(x) - f_\Lambda(x) | f_{\Lambda+d\Lambda}(x) - f_\Lambda(x) \rangle|,$$

$$\langle f(x) | g(x) \rangle = \int_D dx f(x) g(x)$$

$$C = \sum_\Lambda \frac{1}{d\Lambda} \Delta_\Lambda \rightarrow \int |\langle \frac{\partial f}{\partial \Lambda} | \frac{\partial f}{\partial \Lambda} \rangle| d\Lambda, \text{ as } d\Lambda \rightarrow 0$$

Structural complexity II

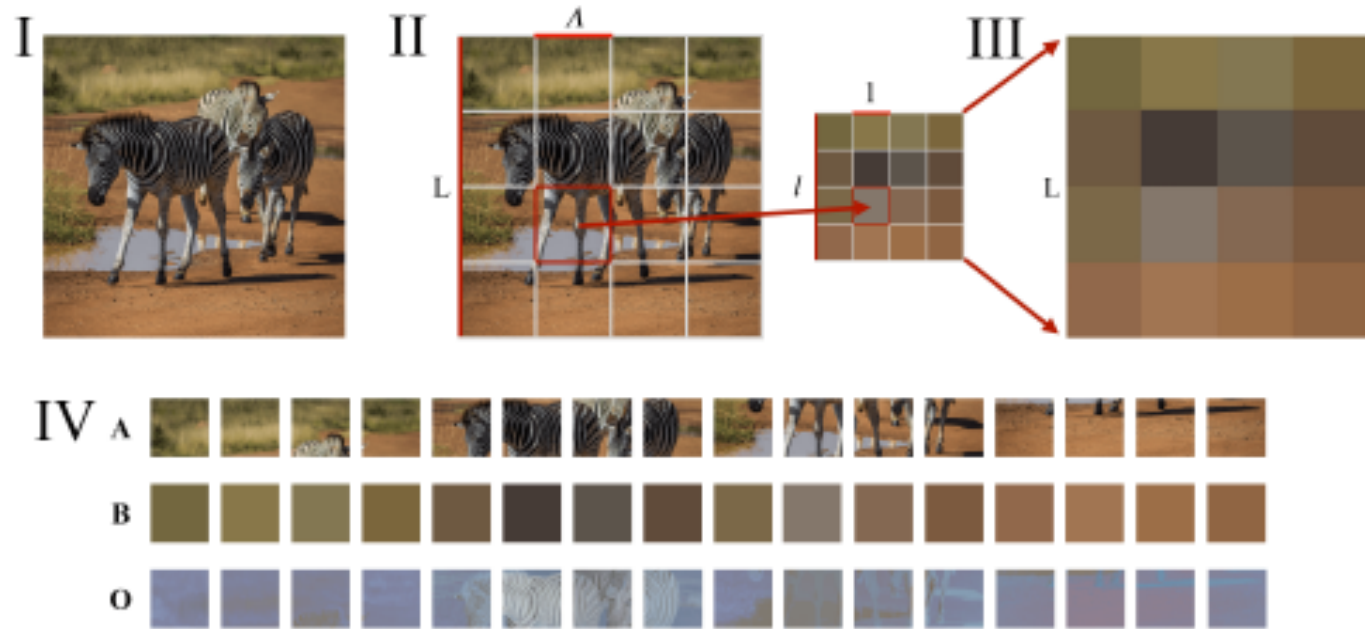
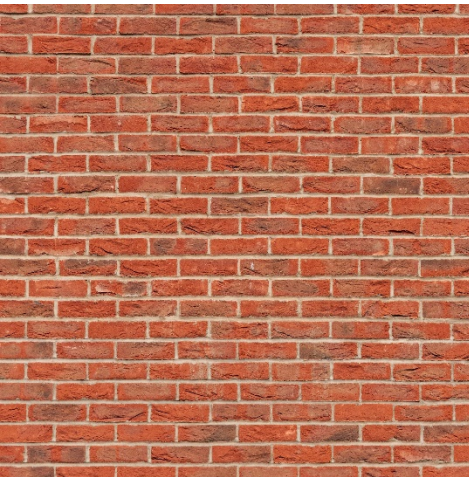
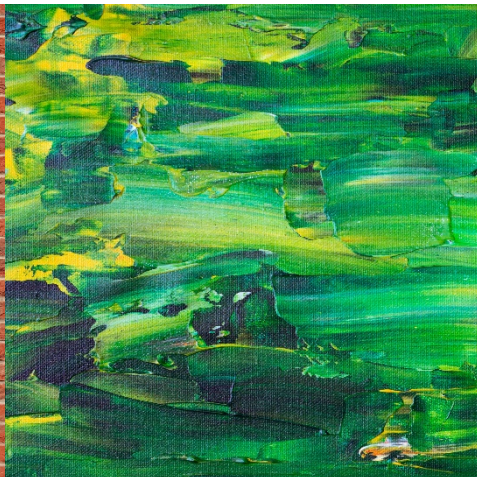


FIG. 1. Schematic representation of the idea behind the proposed method. A photo of $L \times L$ pixels (panel I) taken from www.pexels.com is divided into blocks of $\Lambda \times \Lambda$ pixels (panel II). A renormalized photo of $l \times l$ pixels is plotted, where $l = L/\Lambda$ ($l=4$ in this example). The renormalized photo is rescaled up to initial photo size (panel III). Vectors **A** and **B** are constructed from blocks of the initial and the renormalized images respectively (panel IV). The scalar product of these vectors is used to define overlap O . For illustrative purposes, pixelwise products of **A**- and **B**-blocks are shown as vector **O**.

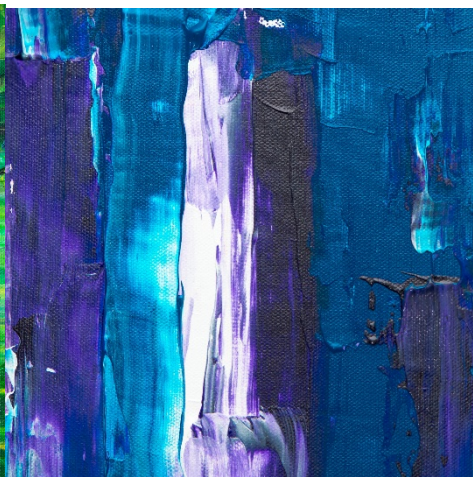
Art objects (and walls)



$C = 0.1076$



$C = 0.2010$



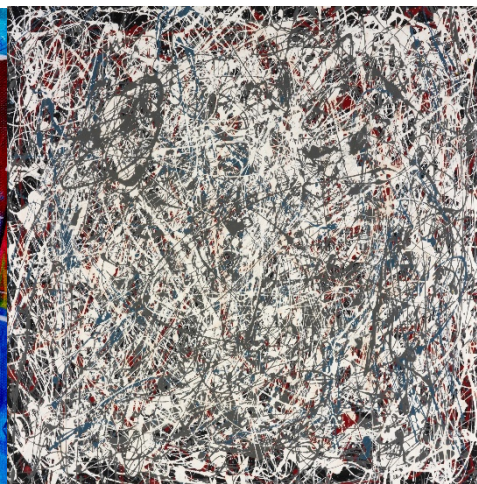
$C = 0.2147$



$C = 0.2765$



$C = 0.4557$



$C = 0.4581$



$C = 0.4975$



$C = 0.5552$

Other objects



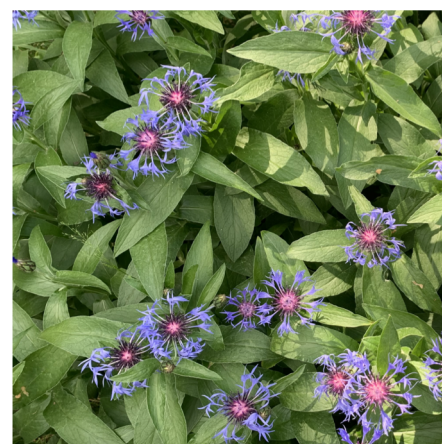
$C = 0.353$



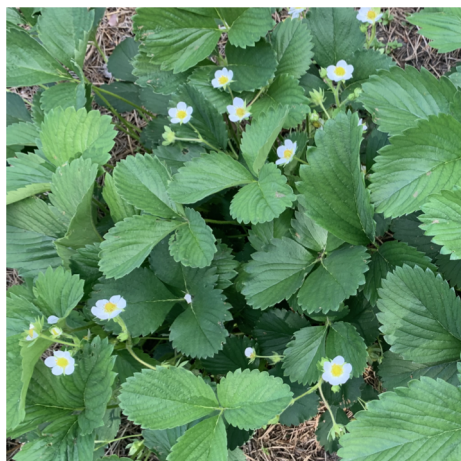
$C = 0.152$



$C = 0.204$



$C = 0.260$



$C = 0.167$



$C = 0.316$



$C = 0.209$

*Photos by V. V.
Mazurenko*

Solution of an ink drop in water

Entropy should grow, but complexity is not! And indeed...

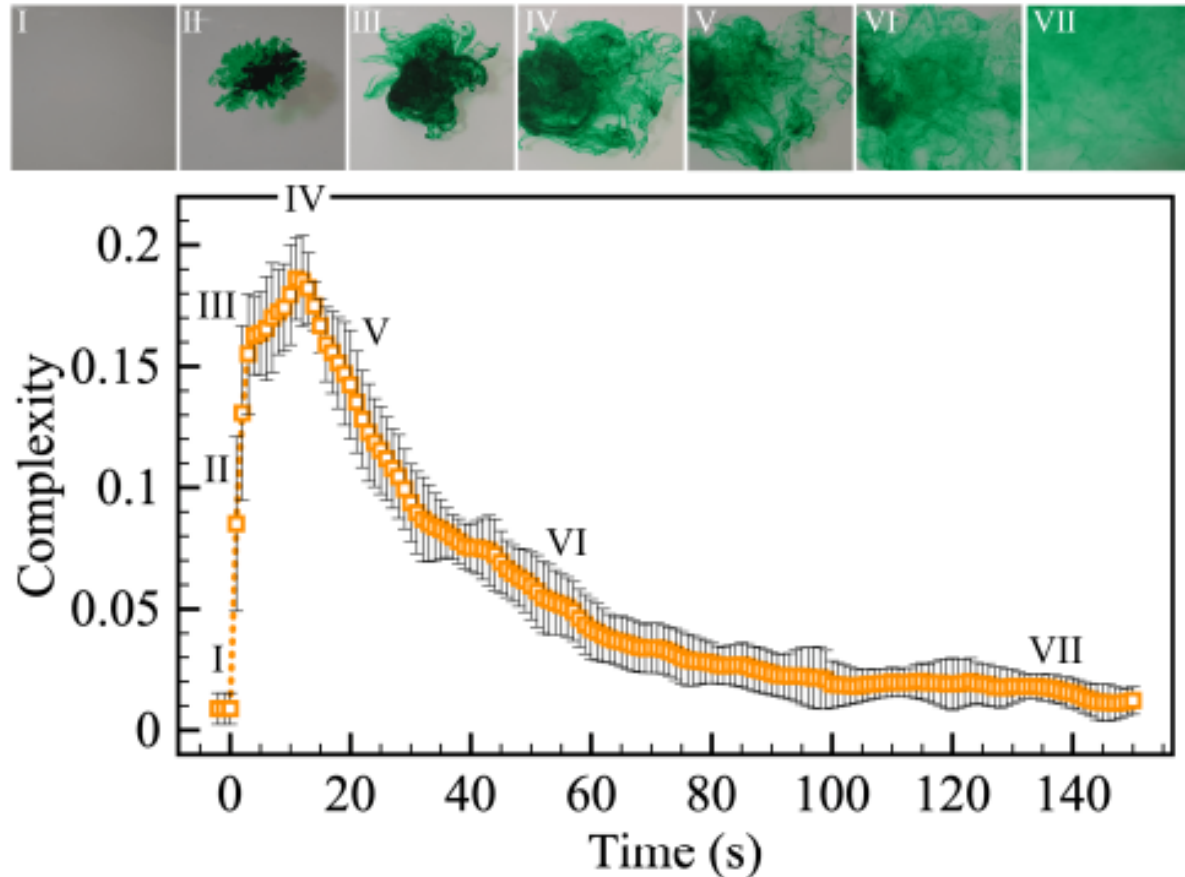


FIG. 7. The evolution of the complexity during the process of dissolving a food dye drop of 0.3 ml in water at 31°C.

Structural complexity: 2D Ising model

Can be used as a numerical tool to find T_C from finite-size simulations

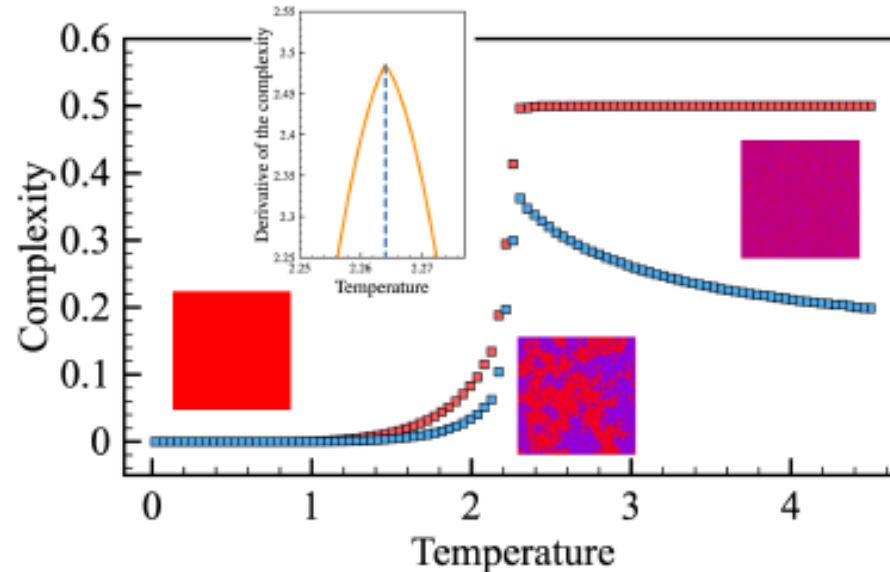


FIG. 2. Temperature dependence of the complexity obtained from the two-dimensional Ising model simulations. Red and blue squares correspond to the complexities calculated with $k \geq 0$ and $k \geq 1$, respectively. The size of error bars is smaller than the symbol size. Inset shows the first derivative of the complexity used for accurate detection of the critical temperature. Here we used $N = 8$, $\Lambda = 2$.

Structural complexity: 3D Ising model

3D Ising model,
cubic lattice
(insert shows
temperature
derivative of
Complexity)

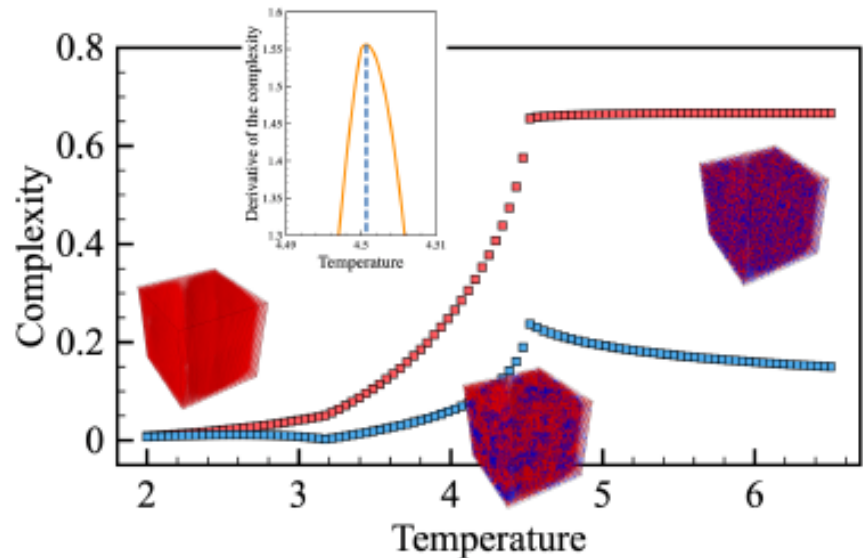


FIG. 3. Temperature dependence of the complexity obtained from the three-dimensional Ising model simulations with $\Lambda = 2$. Red and blue squares correspond to the complexities calculated with $k \geq 0$ and $k \geq 1$, respectively. The size of error bars is smaller than the symbol size. Inset shows the first derivative of the complexity used for accurate detection of the critical temperature. Here we used $L \times L \times L$ cubic lattice with $L = 256$, $N = 6$. The small but visible cusp on the blue curve around $T \simeq 3.2$ reflects the emergence of magnetic domains within the ferromagnetic phase, which takes place sometimes during MC simulations on large lattices.

Structural complexity: Static patterns

Spin textures due to competition of exchange and
Dzialoshinskii-Moriya interactions

$$H = -J \sum_{nn'} \mathbf{S}_n \mathbf{S}_{n'} - \mathbf{D} \sum_{nn'} [\mathbf{S}_n \times \mathbf{S}_{n'}] - \sum_n B S_n^z$$

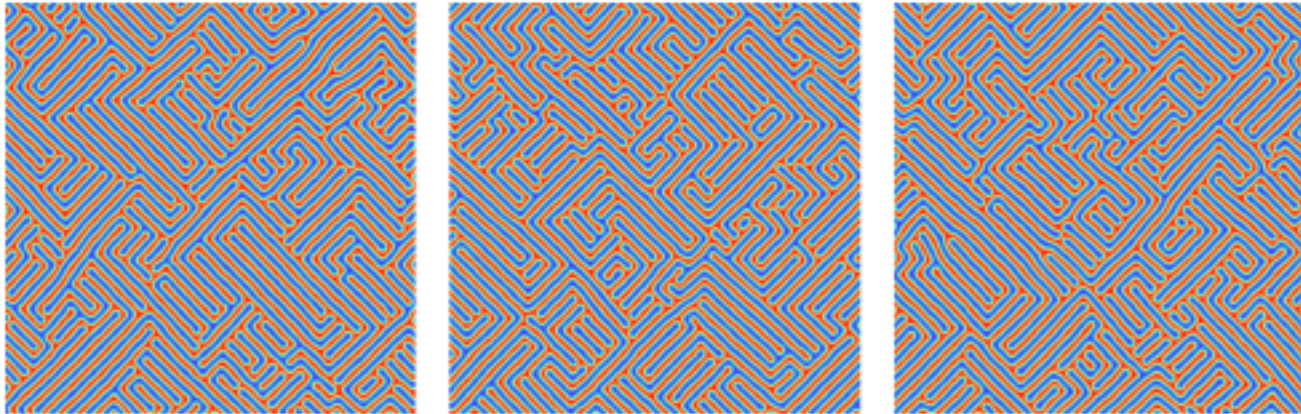


FIG. 5. Configurations of the DM magnetic on 1024×1024 square lattice obtained from independent Monte Carlo runs with parameters $B = 0.05J$, $|\mathbf{D}| = J$, $T = 0.02J$. While they are visually distinct, corresponding complexities (left to right) are equal to $\mathcal{C} = 0.4992115$, $\mathcal{C} = 0.4991825$ and $\mathcal{C} = 0.4991805$.

Structural complexity: Static patterns II

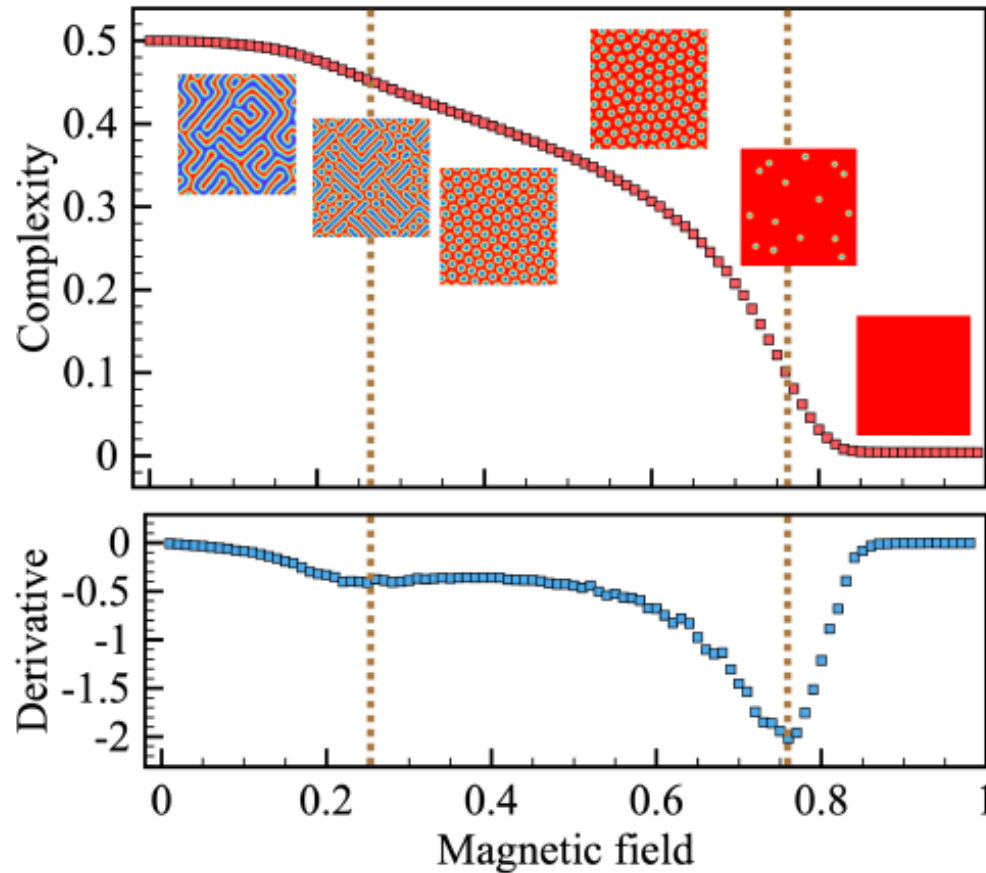


FIG. 4. (a) Magnetic field dependence of the complexity obtained from the simulations with spin Hamiltonian containing DM interaction with $J = 1$, $|D| = 1$, $T = 0.02$. The error bars are smaller than the symbol size. (b) Complexity derivative we used for accurate detection of the phases boundaries.

Complexity in magnets under laser pulses

$$H = -J \sum_{nn'} \mathbf{S}_n \mathbf{S}_{n'} - \mathbf{D} \sum_{nn'} [\mathbf{S}_n \times \mathbf{S}_{n'}] - K \sum_n (\mathbf{S}_n^z)^2$$

$$\begin{aligned} \frac{d\mathbf{S}_n}{dt} = & -\frac{\gamma}{1+\alpha^2} \mathbf{S}_n \times \left[-\frac{\partial H}{\partial \mathbf{S}_n} + b_n(t) \right] - \\ & -\frac{\gamma}{|\mathbf{S}_n|} \frac{\alpha}{1+\alpha^2} \mathbf{S}_n \times (\mathbf{S}_n \times \left[-\frac{\partial H}{\partial \mathbf{S}_n} + b_n(t) \right]), \end{aligned}$$

Nonthermal effect of laser pulses: effective magnetic field (inverse Faraday effect)

$$\mathbf{B}_p(t) = B_0 \exp \left(-\frac{(t - t_p)^2}{2t_w^2} \right) \mathbf{e}_B$$

Complexity in magnets under laser pulses II

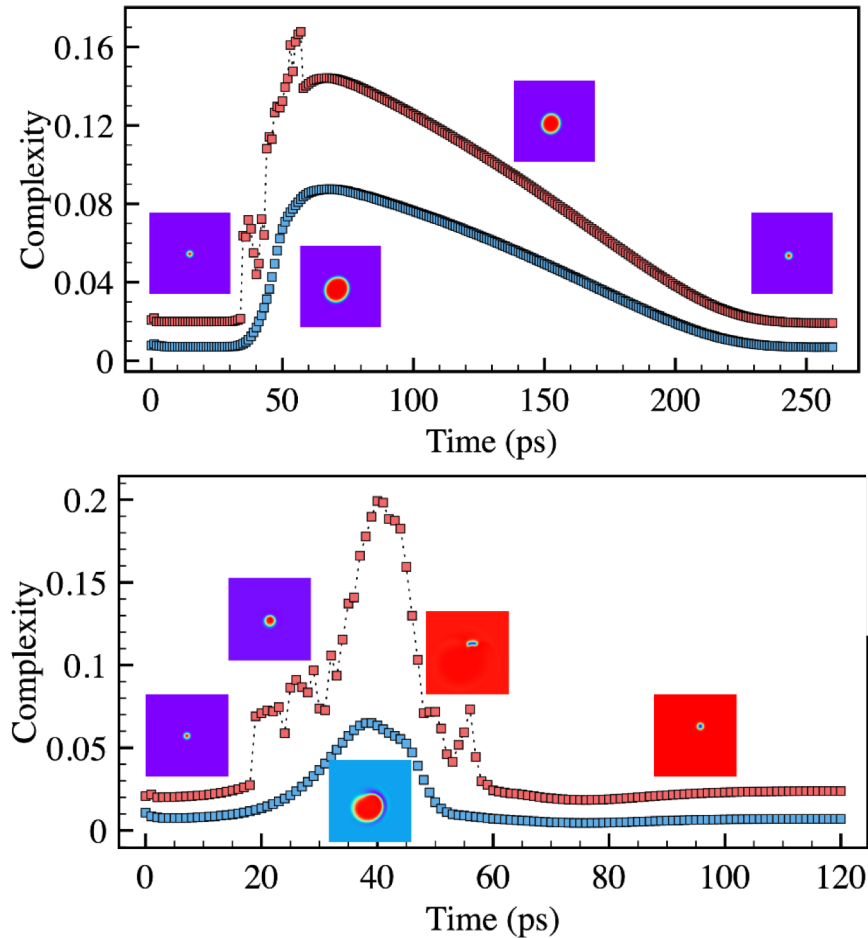


Fig. 11. The evolution of the complexity during the (top panel) breathing and (bottom panel) switching processes generated with $t_w = 8$ ps and $t_w = 28$ ps, respectively. Red and blue squares correspond to the complexities calculated for 2048×2048 images and 128×128 square lattice of Heisenberg spins, respectively.

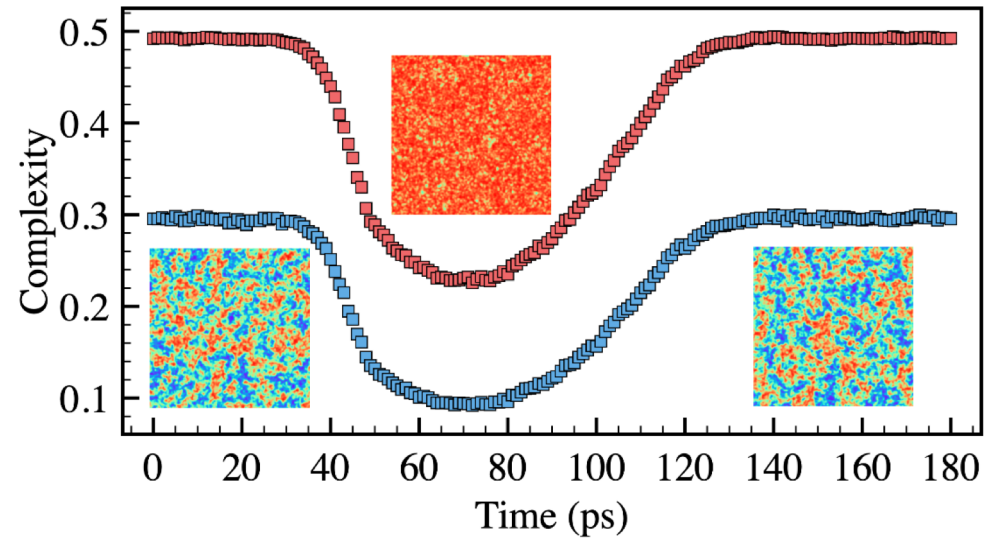


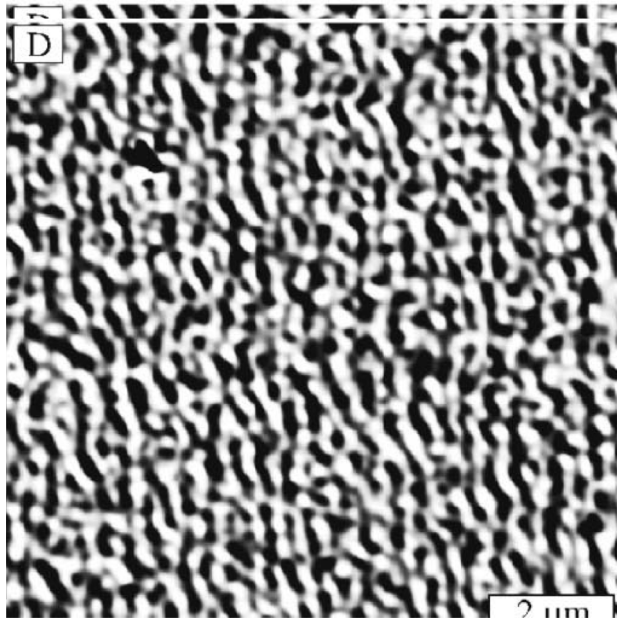
Fig. 12. The evolution of the complexity of the paramagnetic spin configuration at $T = 9$ K under the influence of $t_w = 36$ ps magnetic pulse along z axis. Red and blue squares correspond to the complexities calculated with $k \geq 0$ and $k \geq 1$, respectively. The amplitude of the magnetic pulse is $B_0 = 10$ T.

Competing interactions and self-induced spin glasses

Special class of patterns: “chaotic” patterns

Hypothesis: a system wants to be modulated but cannot decide in which direction

PHYSICAL REVIEW B 69, 064411 (2004)



$$E_m = \int \int d\mathbf{r} d\mathbf{r}' m(\mathbf{r}) m(\mathbf{r}') \left[\frac{1}{|\mathbf{r} - \mathbf{r}'|} - \frac{1}{\sqrt{(\mathbf{r} - \mathbf{r}')^2 + D^2}} \right]$$
$$= 2\pi \sum_{\mathbf{q}} m_{\mathbf{q}} m_{-\mathbf{q}} \frac{1 - e^{-qD}}{q}, \quad (13)$$

where $m_{\mathbf{q}}$ is a two-dimensional Fourier component of the magnetization density. At the same time, the exchange energy can be written as

$$E_{exch} = \frac{1}{2} \alpha \sum_{\mathbf{q}} q^2 m_{\mathbf{q}} m_{-\mathbf{q}}, \quad (14)$$

so there is a finite value of the wave vector $q = q^*$ found from the condition

$$\frac{d}{dq} \left(2\pi \frac{1 - e^{-qD}}{q} + \frac{1}{2} \alpha q^2 \right) = 0 \quad (15)$$

Self-induced spin glasses II

PHYSICAL REVIEW B 93, 054410 (2016)

PRL 117, 137201 (2016)

PHYSICAL REVIEW LETTERS

week ending
23 SEPTEMBER 2016

Stripe glasses in ferromagnetic thin films

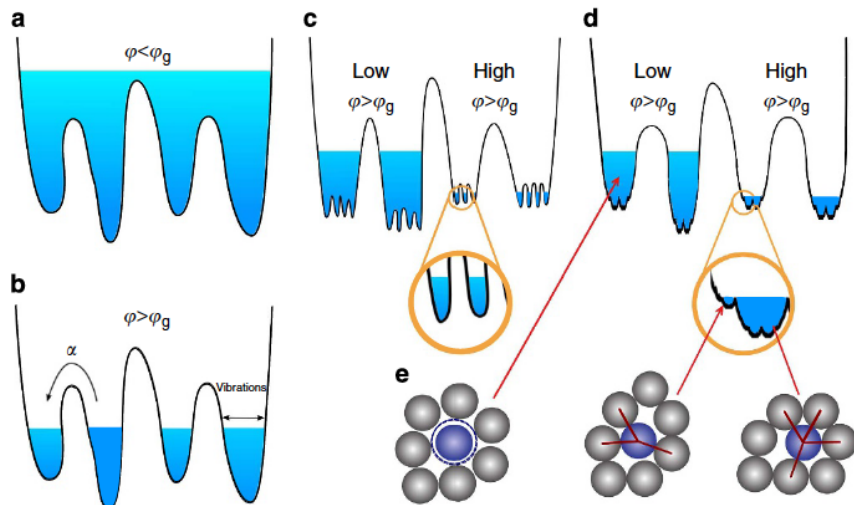
Alessandro Principi* and Mikhail I. Katsnelson

Self-Induced Glassiness and Pattern Formation in Spin Systems Subject to Long-Range Interactions

Alessandro Principi* and Mikhail I. Katsnelson

Development of idea of stripe glass, J. Schmalian and P. G. Wolynes, PRL 2000

Glass: a system with an energy landscape characterizing by infinitely many local minima, with a broad distribution of barriers, relaxation at “any” time scale and **aging** (at thermal cycling you never go back to *exactly* the same state)



Picture from P. Charbonneau et al,

DOI: 10.1038/ncomms4725

Intermediate state between equilibrium and non-equilibrium, opportunity for history and memory (“stamp collection”)

Self-induced spin glasses III

One of the ways to describe: R. Monasson, PRL 75, 2847 (1995)

$$\mathcal{H}_\psi[m, \lambda] = \mathcal{H}[m, \lambda] + g \int dr [m(r) - \psi(r)]^2$$

The second term describes attraction of our physical field $m(r)$
to some external field $\psi(r)$

If the system can be glued, with infinitely small interaction g , to macroscopically large number of configurations it should be considered as a glass

Then we calculate $F_g = \frac{\int \mathcal{D}\psi Z[\psi] F[\psi]}{\int \mathcal{D}\psi Z[\psi]}$ and see whether the limits

$F_{\text{eq}} = \lim_{N \rightarrow \infty} \lim_{g \rightarrow 0} F_g$ and $F = \lim_{g \rightarrow 0} \lim_{N \rightarrow \infty} F_g$ are different

If yes, this is **self-induced glass**

No disorder is needed (contrary to traditional view on spin glasses)

Self-induced spin glasses IV

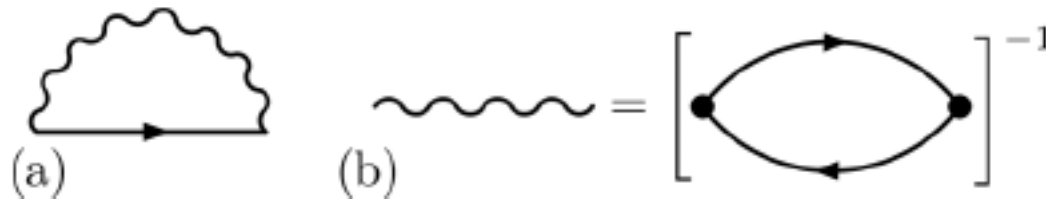
PHYSICAL REVIEW B 93, 054410 (2016)

Stripe glasses in ferromagnetic thin films

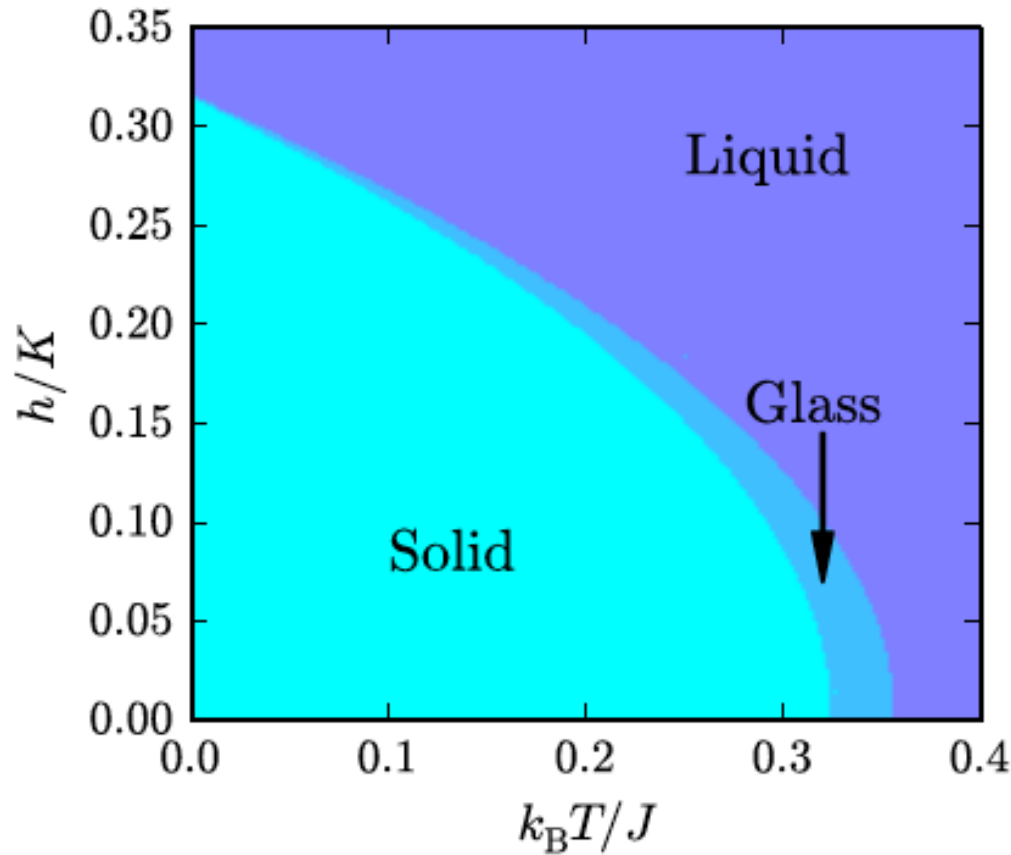
Alessandro Principi* and Mikhail I. Katsnelson

$$\begin{aligned} \mathcal{H}[m, \lambda] = & \int dr \{ J [\partial_i m_j(r)]^2 - K m_z^2(r) - 2h(r) \cdot m(r) \} \\ & + \frac{Q}{2\pi} \int dr dr' m_z(r) \\ & \times \left[\frac{1}{|r - r'|} - \frac{1}{\sqrt{d^2 + |r - r'|^2}} \right] m_z(r') \\ & + \int dr \{ \lambda(r) [m^2(r) - 1] \}. \end{aligned} \quad (1)$$

Self-consistent screening approximation for spin propagators



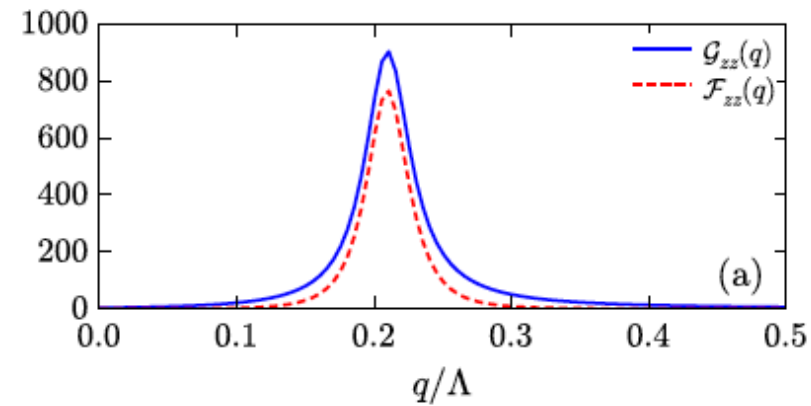
Self-induced spin glasses V



Phase diagram

Maximum at

$$q_0 \simeq [Q/(2J)]^{1/3} \neq 0$$



q -dependence of normal and anomalous (“glassy”, non-ergodic spin-spin correlators

Self-induced spin glasses VI

PRL 117, 137201 (2016)

PHYSICAL REVIEW LETTERS

week ending
23 SEPTEMBER 2016

Self-Induced Glassiness and Pattern Formation in Spin Systems Subject to Long-Range Interactions

Alessandro Principi* and Mikhail I. Katsnelson

Maximal simplification
(Brazovskii model)

$$\mathcal{F} = \frac{1}{2} \sum_{\mathbf{q}} G_0^{-1}(\mathbf{q}) s_{\mathbf{q}} \cdot s_{-\mathbf{q}} + i \sum_i \sigma_i (s_i^2 - 1)$$

$$G_0^{-1}(\mathbf{q}) = q_0^D (q^2 / q_0^2 - 1)^2 / 4 + q_0^D \varepsilon_0^2 \sin^2(\theta_q)$$

Spin-glass state exists!

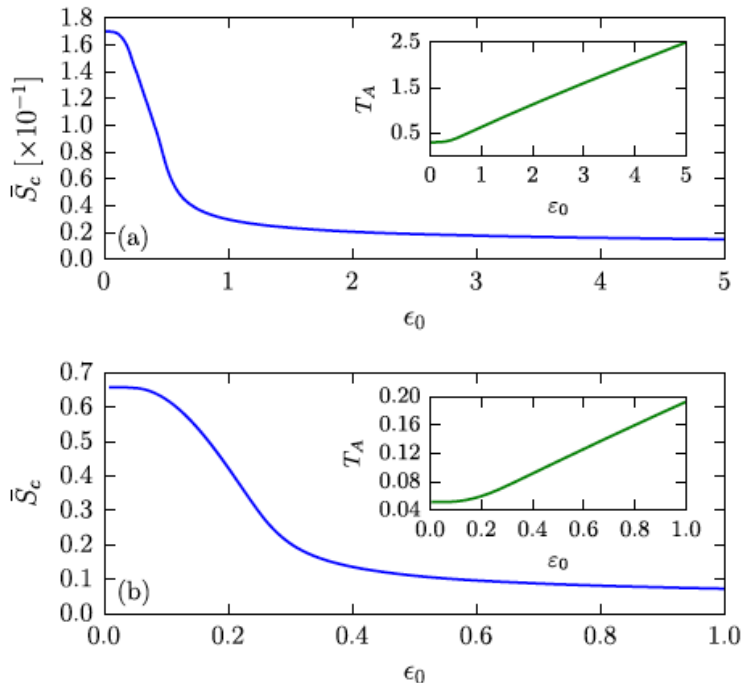


FIG. 2. Panel (a) the configurational entropy of the mean-field problem for the two-dimensional Ising model ($D=2$ and $N_s=1$). Note that this curve has been multiplied by a factor 0.1. Inset: the transition temperature T_A as a function of the anisotropy parameter ϵ_0 . Panel (b) same as panel (a) but for the two-dimensional Heisenberg model ($D=2$, $N_s=3$). Inset: the temperature T_A as a function of ϵ_0 .

Experimental observation of self-induced spin glass state: elemental Nd

Self-induced spin glass state in elemental and crystalline neodymium

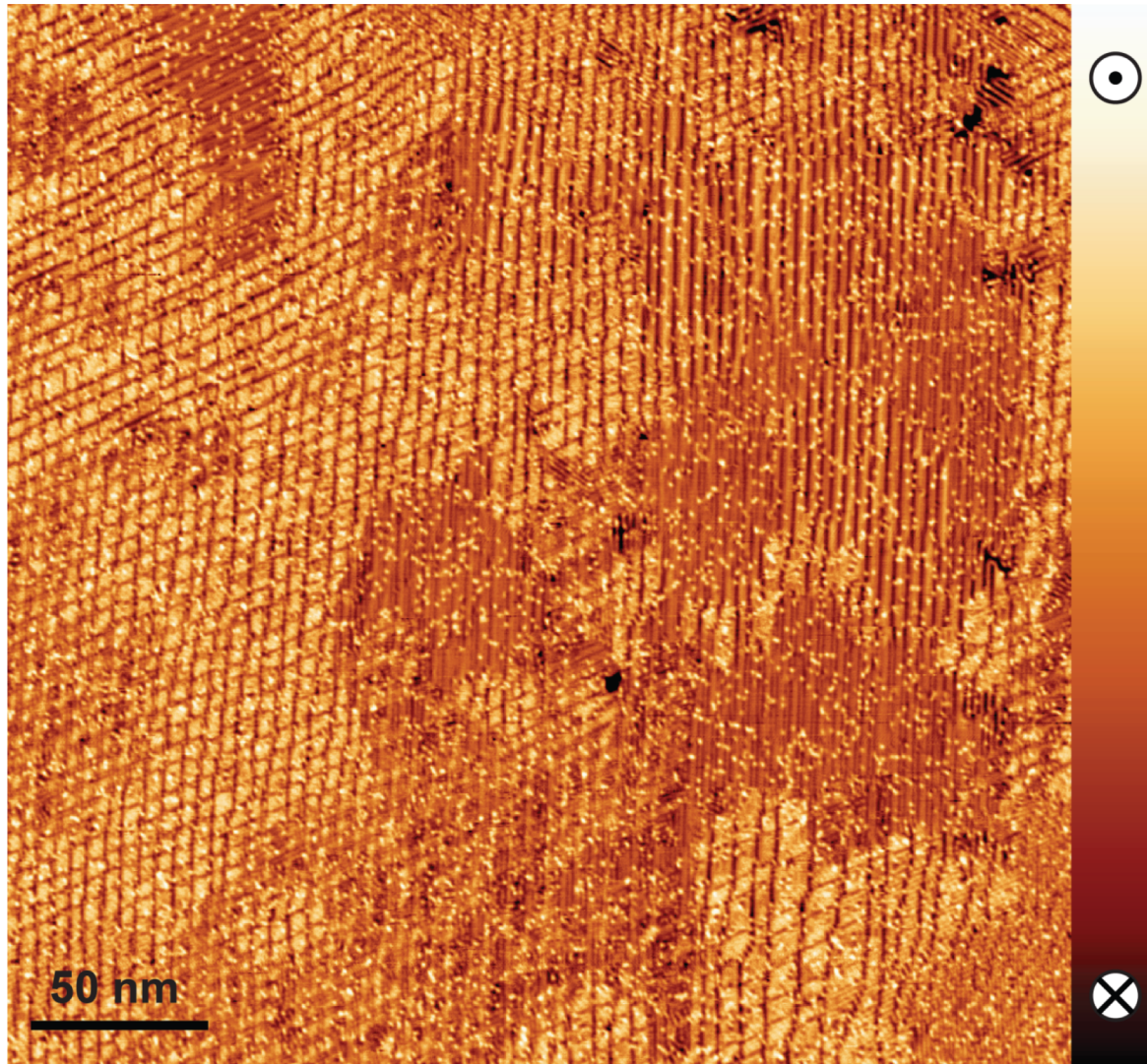
Science **368**, 966 (2020)

Umut Kamber, Anders Bergman, Andreas Eich, Diana Iuşan, Manuel Steinbrecher, Nadine Hauptmann, Lars Nordström, Mikhail I. Katsnelson, Daniel Wegner*, Olle Eriksson, Alexander A. Khajetoorians*

Spin-polarized STM experiment, Radboud University



Magnetic structure: no long-range

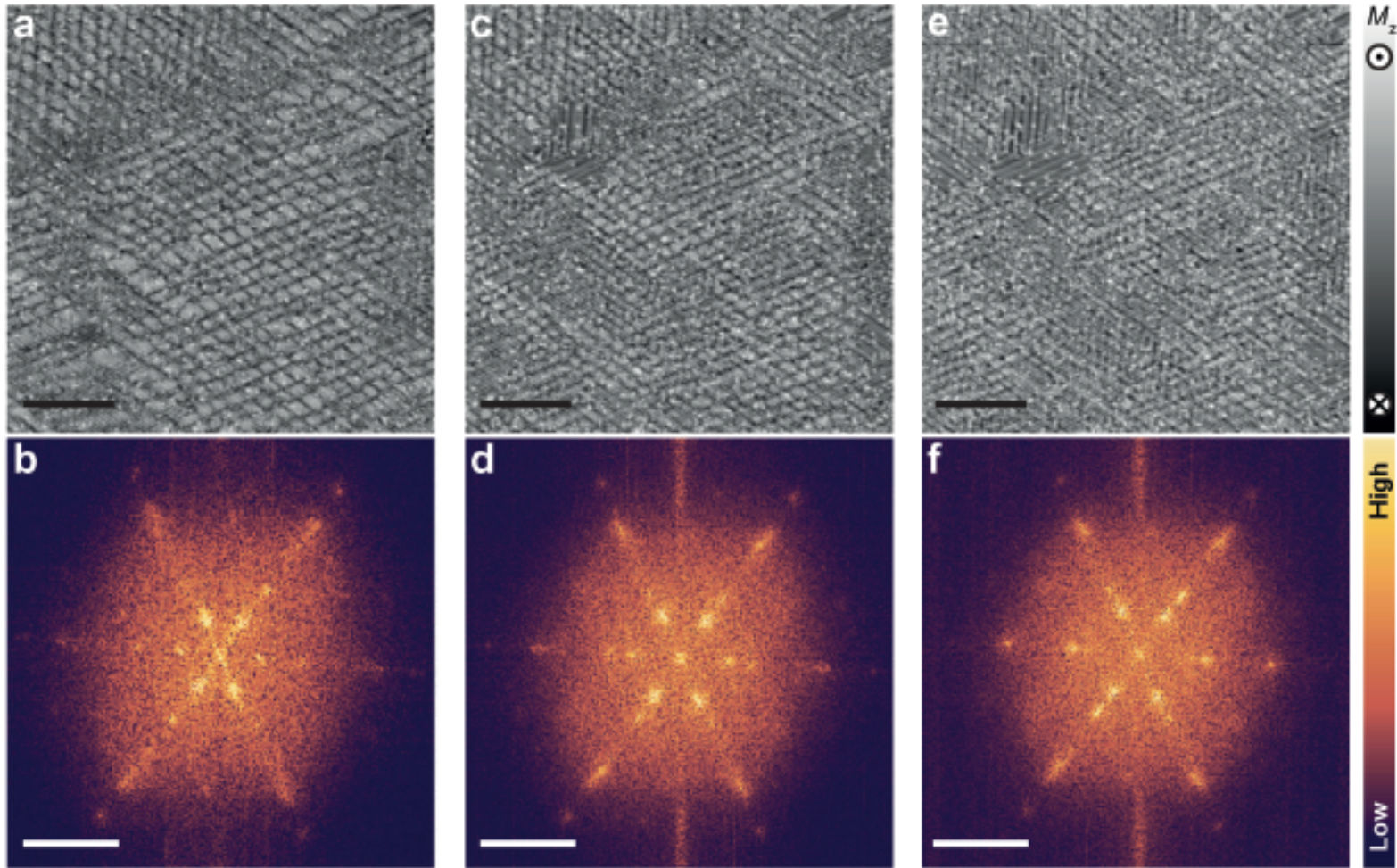


- ✓ Short-range non-collinear order
- ✗ Long-range order

Cr bulk tip

$T: 1.3K$
 $B: 0T$

Magnetic structure: local correlations

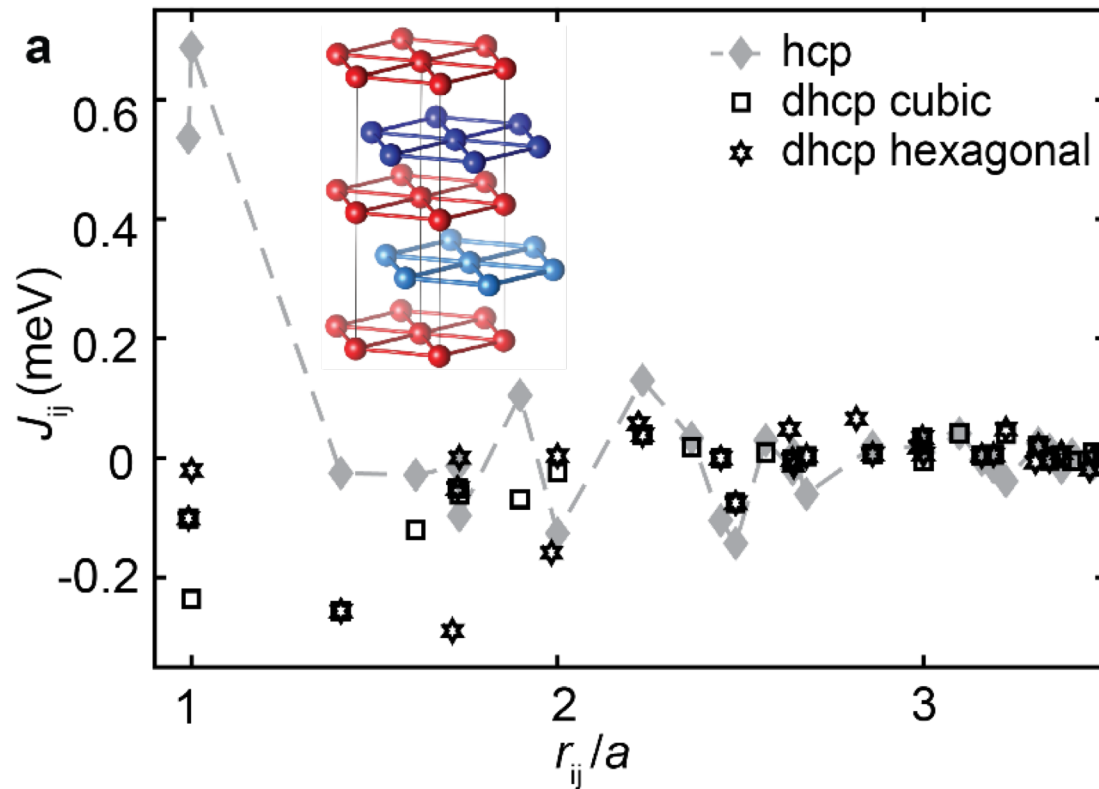


The most important observation: **aging**. At thermocycling (or cycling magnetic field) the magnetic state is not exactly reproduced

Ab initio: magnetic interactions in bulk Nd

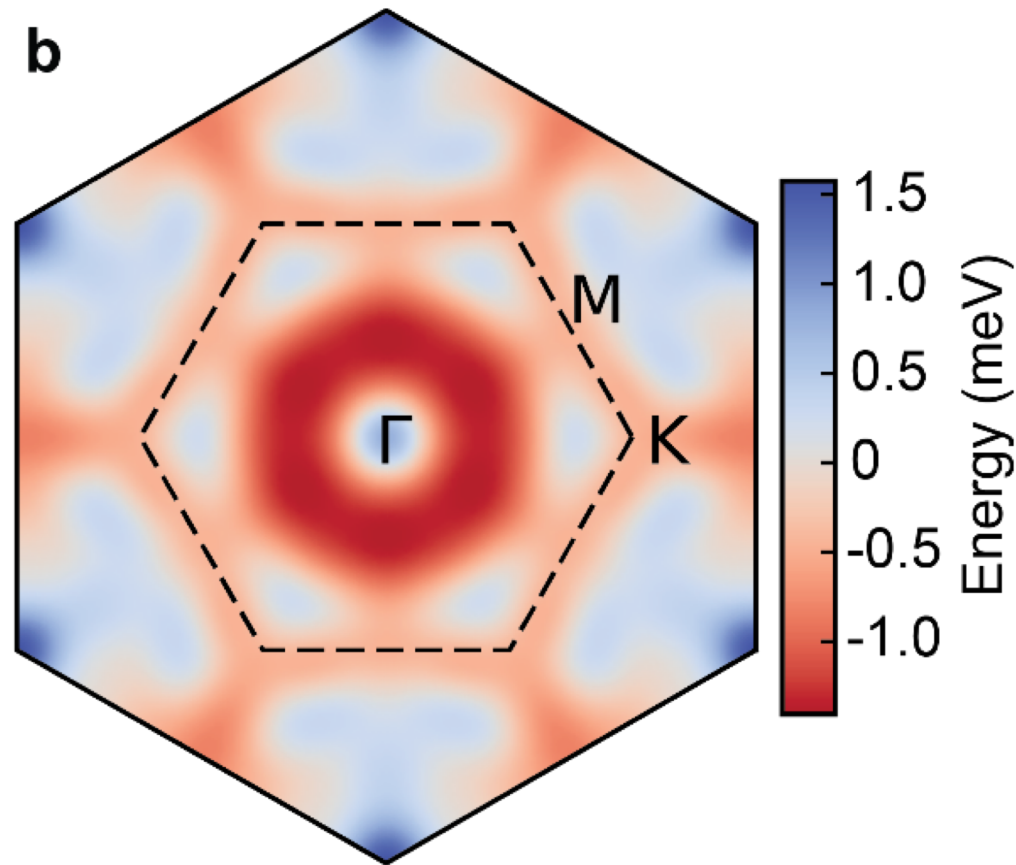
Method: magnetic force theorem (Lichtenstein, Katsnelson, Antropov, Gubanov
JMMM 1987)

Calculations: Uppsala team (Olle Eriksson group)



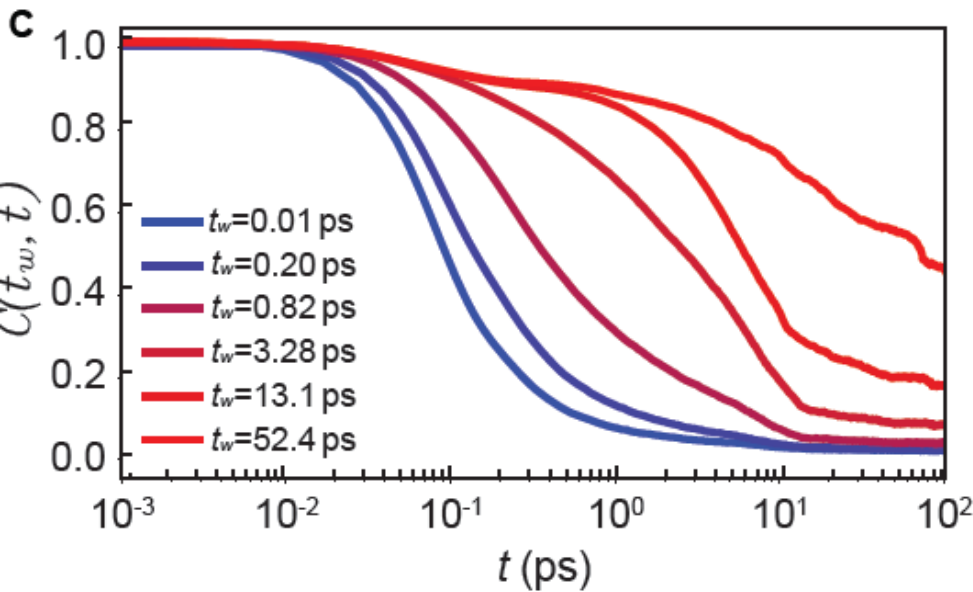
- Dhcp structure drives competing AFM interactions
- Frustrated magnetism

Ab initio bulk Nd: energy landscape



- $E(Q)$ landscape features flat valleys along high symmetry directions

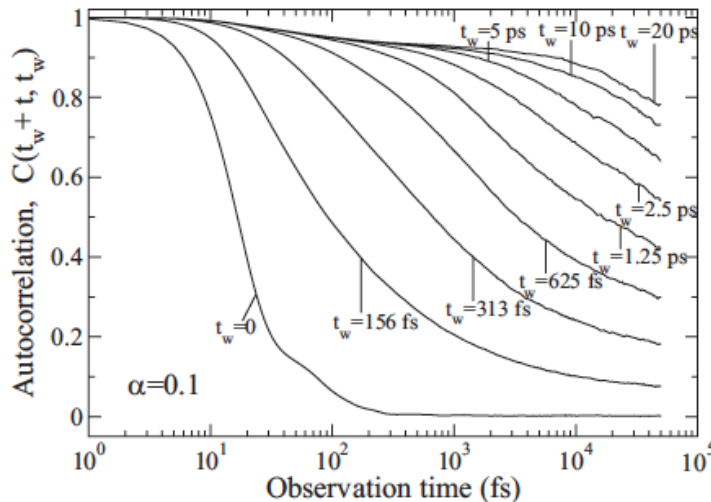
Spin-glass state in Nd: spin dynamics



Atomistic spin dynamics
simulations

Typically spin-glass
behavior

Autocorrelation function $C(t_w, t) = \langle \mathbf{m}_i(t + t_w) \cdot \mathbf{m}_i(t_w) \rangle$ for dhcp Nd at $T = 1$ K



To compare: the same for prototype
disordered spin-glass Cu-Mn

B. Skubic et al, PRB 79, 024411 (2009)

Order from disorder

Thermally induced magnetic order from glassiness in elemental neodymium

NATURE PHYSICS | VOL 18 | AUGUST 2022 | 905-911

Benjamin Verlhac¹, Lorena Niggli¹, Anders Bergman², Umut Kamber¹, Andrey Bagrov^{1,2}, Diana Lușan², Lars Nordström², Mikhail I. Katsnelson¹, Daniel Wegner¹, Olle Eriksson^{2,3} and Alexander A. Khajetoorians¹✉

Glassy state at low T
and long-range order
at T increase

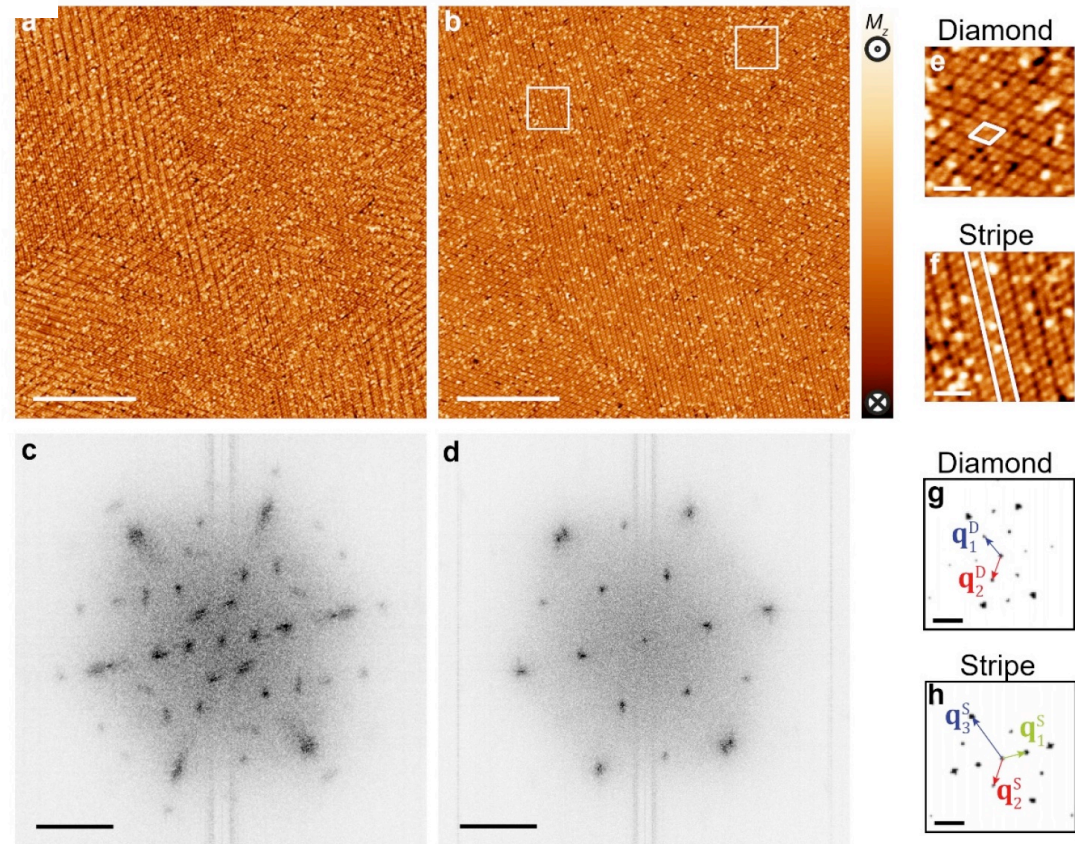
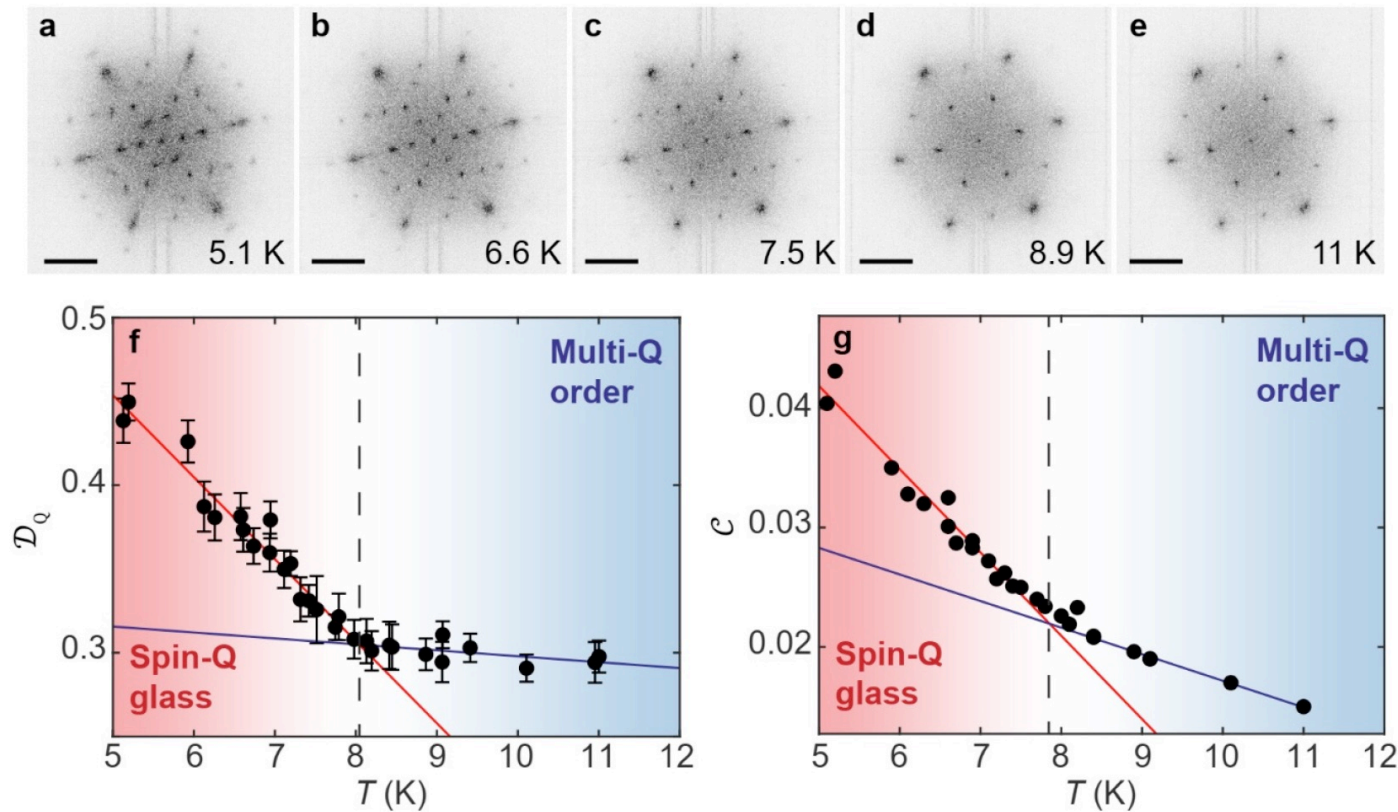


Figure 2: Emergence of long-range multi-Q order from the spin-Q glass state at elevated temperature. a,b. Magnetization images of the same region at $T = 5.1$ K and 11 K, respectively ($I_t = 100$ pA, a-b, scale bar: 50 nm). c,d. Corresponding Q-space images (scale bars: 3 nm⁻¹), illustrating the changes from strong local (i.e. lack of long-range) Q order toward multiple large-scale domains with well-defined long-range multi-Q order. e,f. Zoom-in images of the diamond-like (e) and stripe-like (f) patterns (scale bar: 5 nm). The locations of these images is shown by the white squares in b. g,h. Display of multi-Q state maps of the two apparent domains in the multi-Q ordered phase, where (g)

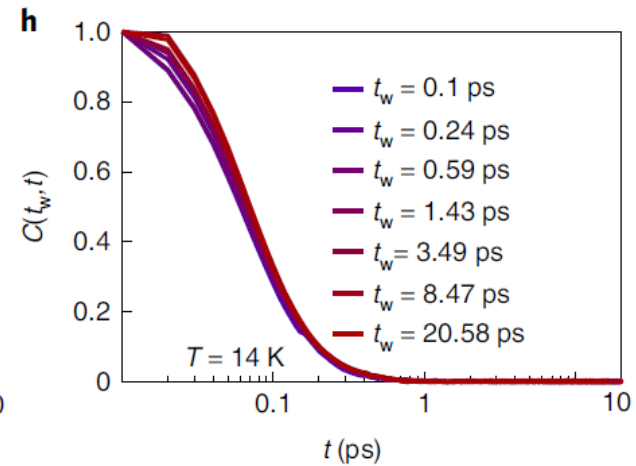
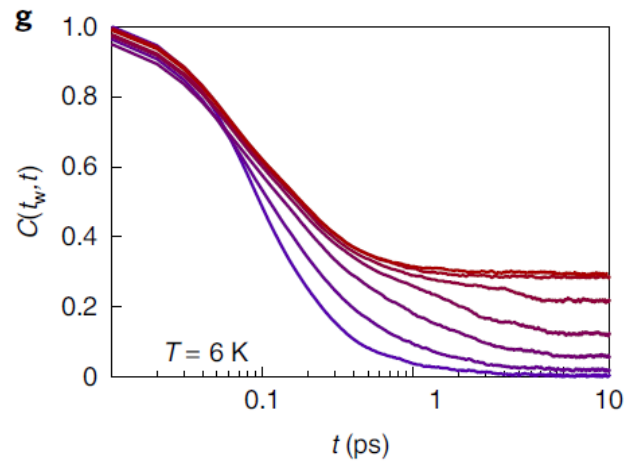
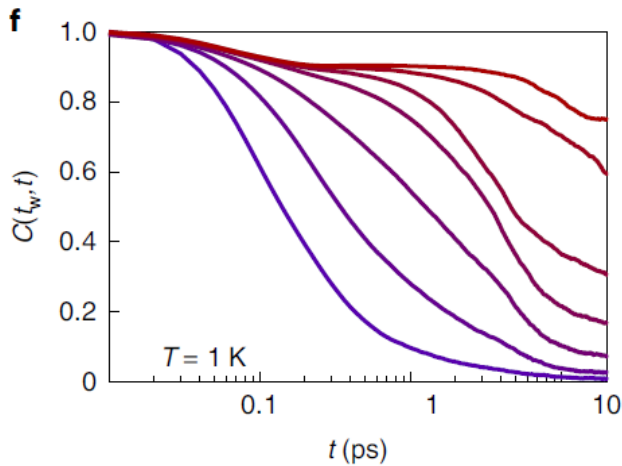
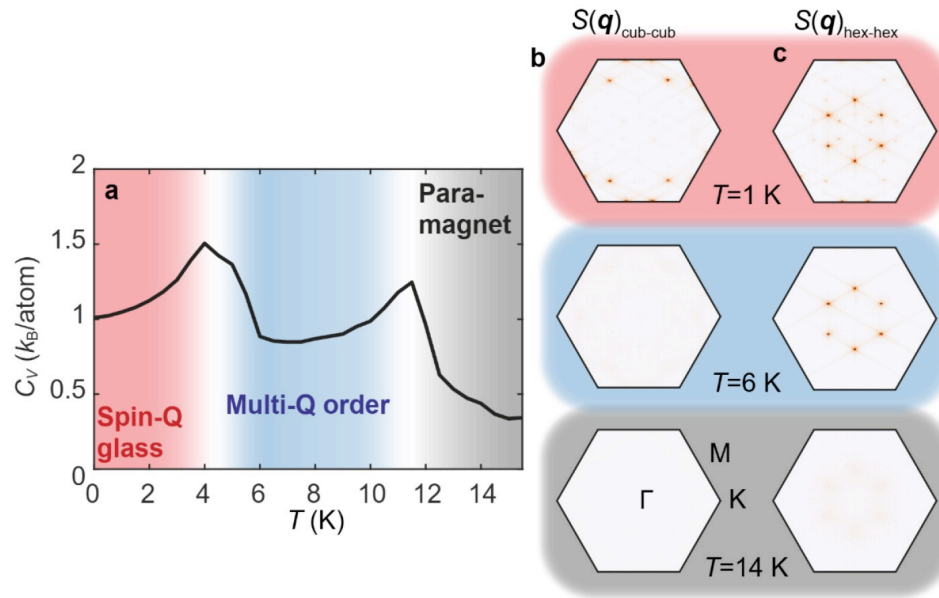
$T=5$ K (a,c): spin glass
 $T=11$ K(b,d): (noncollinear) AFM

Order from disorder II



Phase transition at approx. 8K (seen via “complexity” measures)

Order from disorder III



Theory: Atomistic simulations

Does self-induced glassiness solve the problem?

No! There is no real memory in spin glasses: too many local minima, too small basin of attraction of each minimum

A hypothesis (MIK, Y. Wolf, E. Koonin, Phys. Scr. 93 (2018) 043001):
States that an “glue” not to maroscopically large number of configurations (like in glasses) and not just to a few (like for conventional broken symmnetry) but something in between:




$$H[\phi(x)] \rightarrow H_g[\phi(x)] = H[\phi(x)] + \frac{g}{2} \int dx [\phi(x) - \sigma(x)]^2 \quad \lim_{g \rightarrow +0} \lim_{V \rightarrow \infty} \frac{F_g}{V} \neq \lim_{V \rightarrow \infty} \lim_{g \rightarrow +0} \frac{F_g}{V}$$

for many, but not too many configurations $\sigma(x)$

(in the context of “physical mechanisms of biological evolution”)

Multi-well “memory” state in Ising spin systems

Atom-by-atom construction of attractors in a tunable finite size spin array

A Kolmus¹, M I Katsnelson² , A A Khajetoorians²  and H J Kappen¹ 

New J. Phys. 22 (2020) 023038

2D Ising model, square lattice, no disorder but frustrations due to oscillating character of exchange interactions (2D RKKY)

$$H = - \sum_{i>j} J_{ij} s_i s_j,$$

$$J_{ij} = \begin{cases} 0 & , i = j \\ \frac{1}{r_{ij}^2} \sin\left(\frac{2\pi}{\lambda} r_{ij}\right) & , i \neq j \end{cases}$$

the ratio $\alpha = \lambda/a$ between the RKKY wavelength (λ) and the lattice constant (a)
is the only relevant parameter in the model

Multi-well “memory” state in spin systems II

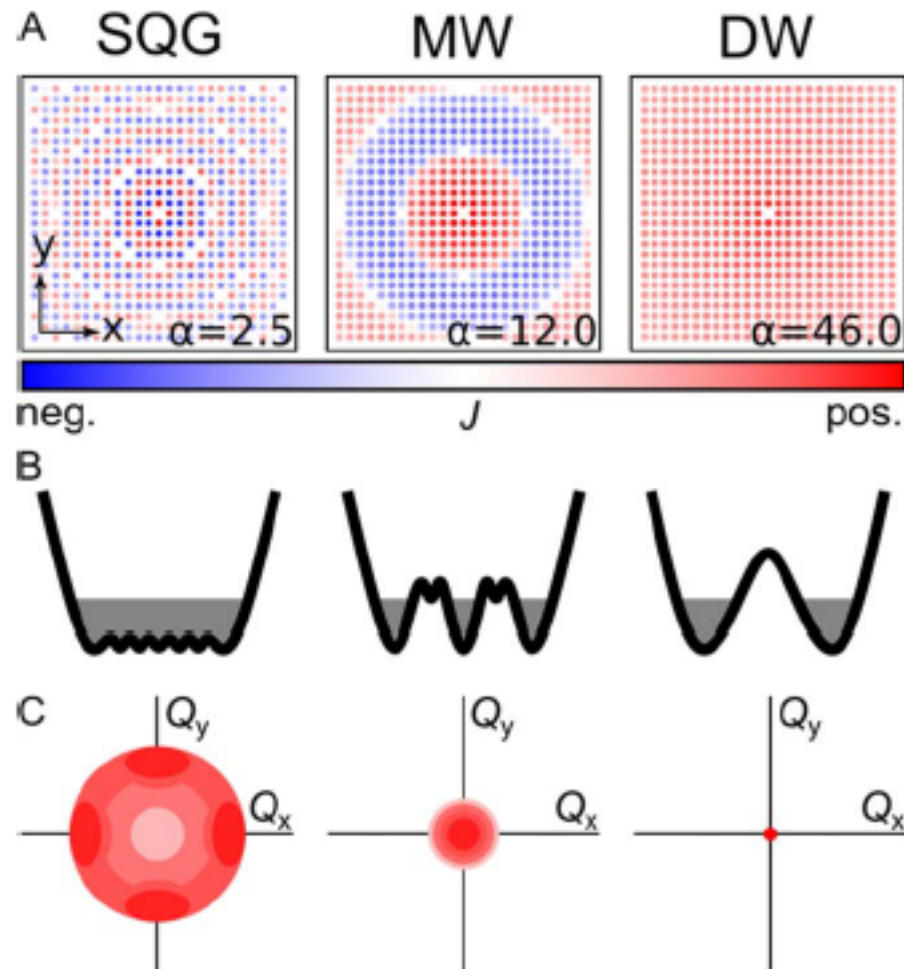


Figure 1. (a) The spatial distribution of the RKKY exchange interaction (J) for the central atom in the Ising spin array ($n = 25$) for different α for the labeled magnetic regime: spin-Q glass (SQG), multi-well (MW), double well (DW). The color bar represents the amplitude and sign of the interaction. (b) Schematic of the energy landscape for the three-labeled regimes, illustrating qualitatively the distribution and depth of states for each regime where gray illustrates the effective temperature. (c) Illustration of the distinguishing features in the Q -space histogram identifying each regime, where white to red intensity corresponds to a low to high number of states.

Multi-well “memory” state in spin systems III

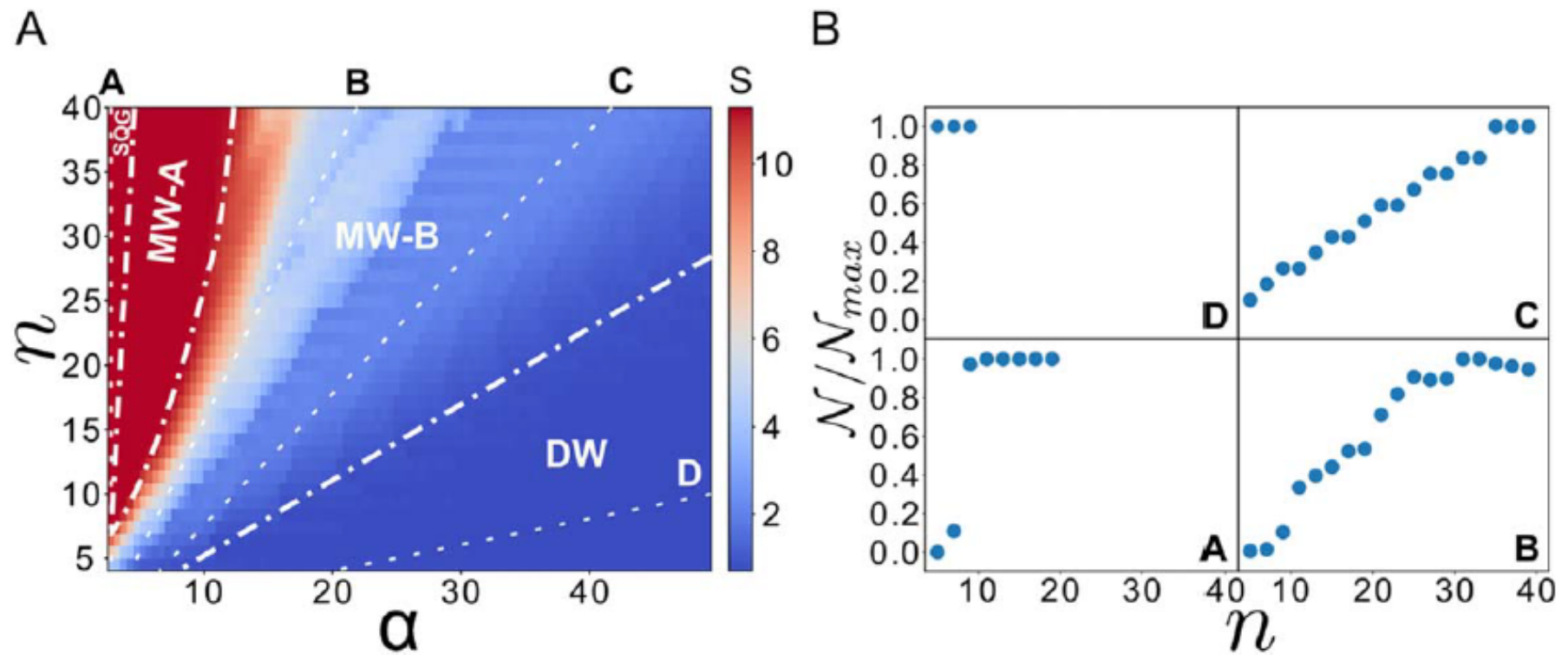


Figure 4. (a) A regime diagram with the lattice width n on the vertical axis and α on the horizontal axis. The white dashed-dot lines indicate the different regimes, as labeled and as defined by the corresponding Q -histograms. The color scale indicates the entropy as defined in the main text. (b) The scaling behavior near the boundary between each regime, corresponding to the white dashed lines in (a) and labeled by the letters A–D. Each plot corresponds to the number of available states as a function of the lattice width n versus the normalized number of metastable states N/N_{\max} . N , N_{\max} are the number of stable states and the largest number of stable states per graph, respectively, and we divide the former by the latter in order to normalize each plot for comparison. These simulations were repeated three times, no large differences were found.

Frustrations and complexity: Quantum case

Generalization properties of neural network
approximations to frustrated magnet ground states

NATURE COMMUNICATIONS | (2020)11:1593

Tom Westerhout¹, Nikita Astrakhantsev^{2,3,4}, Konstantin S. Tikhonov^{5,6,7}, Mikhail I. Katsnelson^{1,8} & Andrey A. Bagrov^{1,8,9}

How to find true ground state of the quantum system?

In general, a very complicated problem (difficult to solve even for quantum computer!)

Idea: use of variational approach and train neural network to find “the best” trial function (G. Carleo and M. Troyer, Science 355, 602 (2017))

$$|\Psi_{\text{GS}}\rangle = \sum_{i=1}^K \psi_i |\mathcal{S}_i\rangle = \sum_{i=1}^K s_i |\psi_i| |\mathcal{S}_i\rangle$$

Generalization problem: to train NN for relatively small basis (K much smaller than total dim. of quantum space) and find good approximation to the true ground state

Frustrations and complexity: Quantum case II

Quantum $S=1/2$ Hamiltonian
NN and NNN interactions

$$\hat{H} = J_1 \sum_{\langle a,b \rangle} \hat{\sigma}_a \otimes \hat{\sigma}_b + J_2 \sum_{\langle\langle a,b \rangle\rangle} \hat{\sigma}_a \otimes \hat{\sigma}_b$$

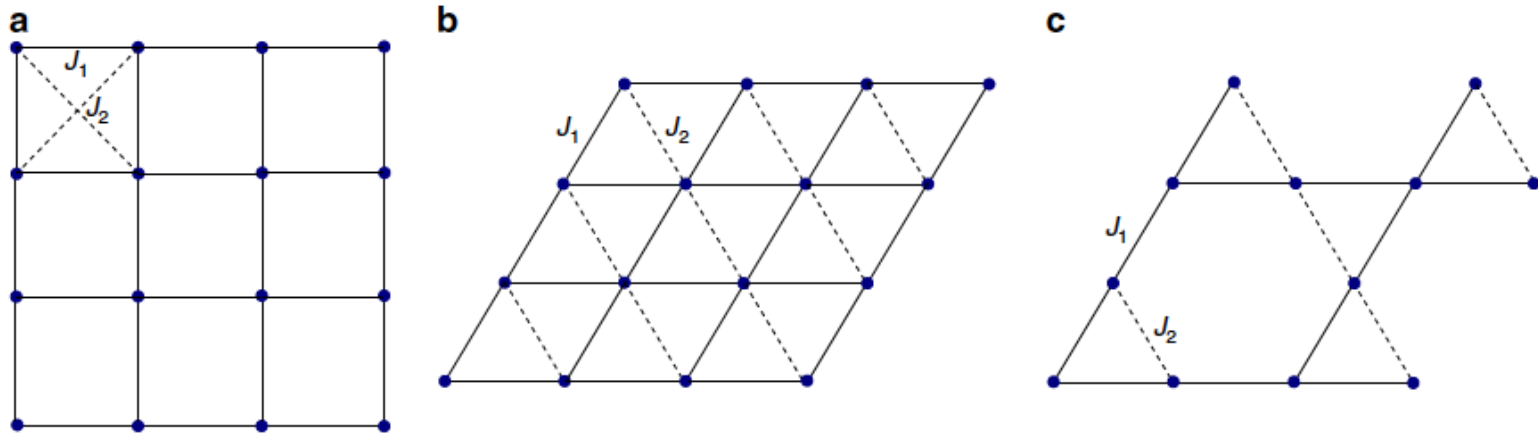


Fig. 1 Lattices considered in this work. We studied three frustrated antiferromagnetic Heisenberg models: **a** next-nearest neighbor J_1 – J_2 model on square lattice; **b** anisotropic nearest-neighbor model on triangular lattice; **c** spatially anisotropic Kagome lattice. In all cases $J_2 = 0$ corresponds to the absence of frustration.

24 spins, dimensionality of Hilbert space $d = C_{12}^{24} \simeq 2.7 \cdot 10^6$

Still possible to calculate ground state exactly
Training for $K = 0.01 d$ (small trial set)

Frustrations and complexity: Quantum case III

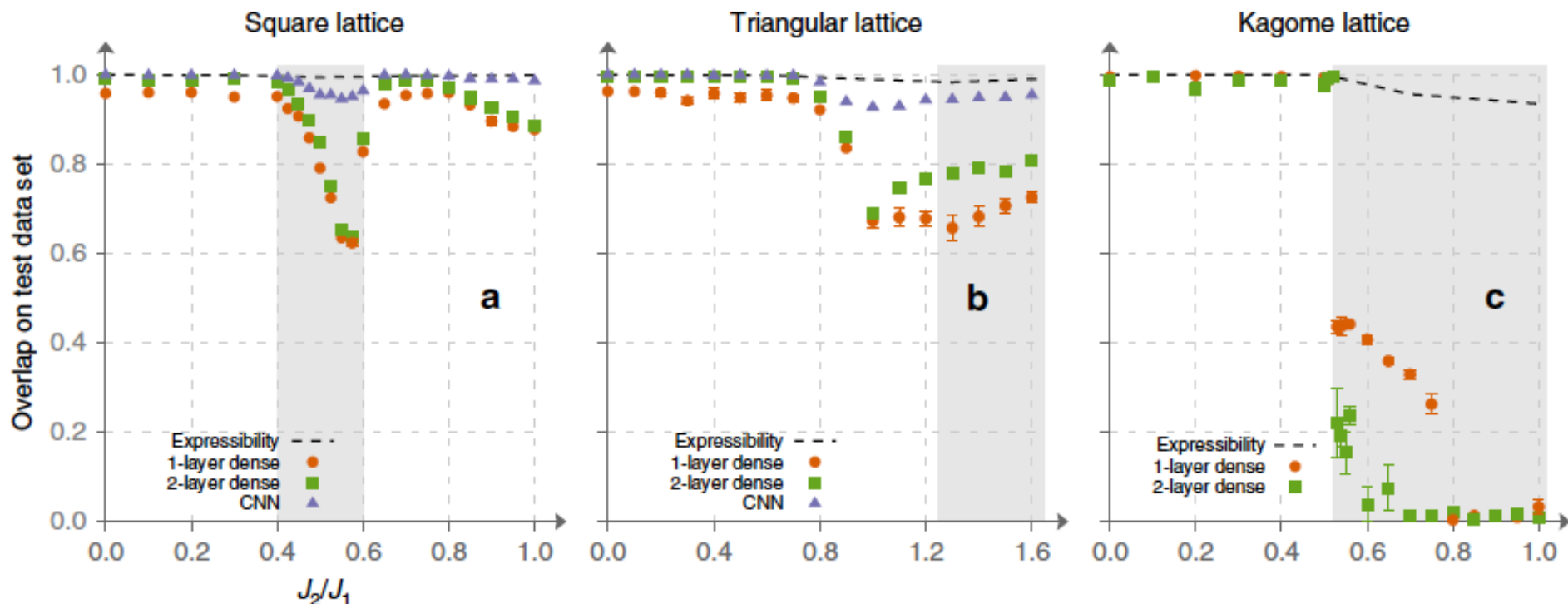
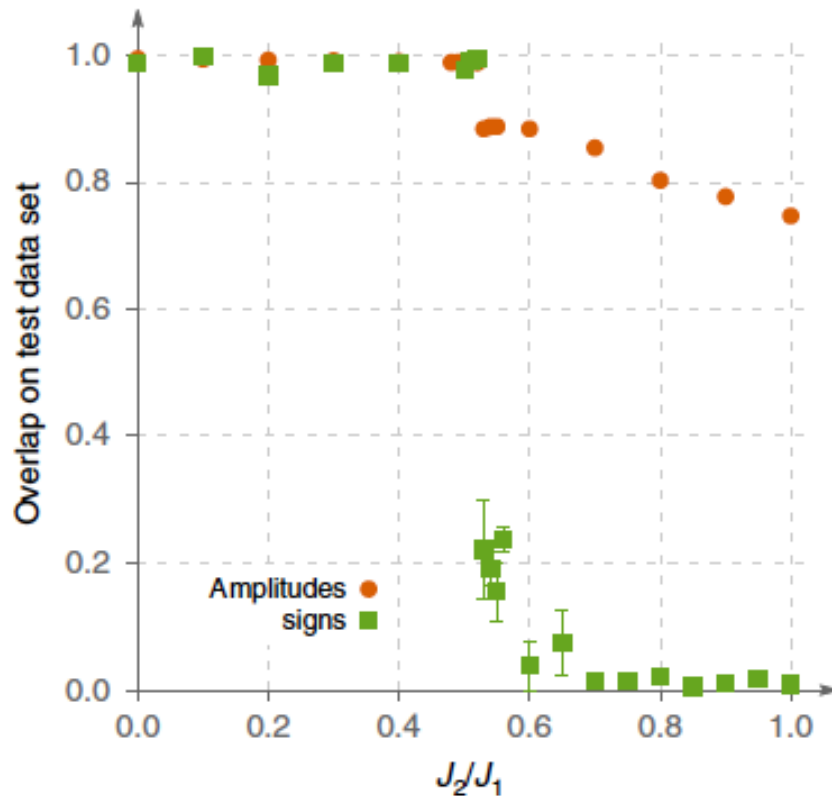


Fig. 2 Optimization results for 24-site clusters obtained with supervised learning and stochastic reconfiguration. Subfigures a-c were obtained using supervised learning of the sign structure. Overlap of the variational wave function with the exact ground state is shown as function of J_2/J_1 for square a, triangular b, and Kagome c lattices. Overlap was computed on the test dataset (not included into training and validation datasets). Note that generalization is poor in the frustrated regions (which are shaded on the plots). 1-layer dense, 2-layer dense, and convolutional neural network (CNN) architectures are described in Supplementary Note 1. Subfigures d-f show overlap between the variational wave function optimized using Stochastic Reconfiguration and the exact ground state for square, triangular, and Kagome lattices, respectively. Variational wave function was represented by two two-layer dense networks. A correlation between generalization quality and accuracy of the SR method is evident. On this figure, as well as on all the subsequent ones (both in the main text and Supplementary Notes 1 and 2), error bars represent standard error (SE) obtained by repeating simulations multiple times.

Frustrations and complexity: Quantum case IV



It is *sign* structure which is difficult to learn in frustrated case!!!

Relation to sign problem in QMC?!

Fig. 4 Generalization of signs and amplitudes. We compare generalization quality as measured by overlap for learning the sign structure (red circles) and amplitude structure (green squares) for 24-site Kagome lattice for two-layer dense architecture. Note that both curves decrease in the frustrated region, but the sign structure is much harder to learn.

"Somehow it seems to fill my head with ideas –only I don't exactly know what they are!" (Through the Looking-Glass, and What Alice Found There)

Further development

Many-body quantum sign structures as non-glassy Ising models

Tom Westerhout, Mikhail I. Katsnelson, Andrey A. Bagrov

[*Communications Physics*](#) volume 6, Article number: 275 (2023)

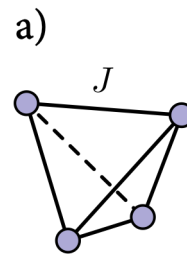
The idea: use machine learning to find amplitudes and then map onto efficient Ising model

$$|\Psi_{\text{GS}}\rangle = \sum_{i=1}^K \psi_i |\mathcal{S}_i\rangle = \sum_{i=1}^K s_i |\psi_i| |\mathcal{S}_i\rangle$$

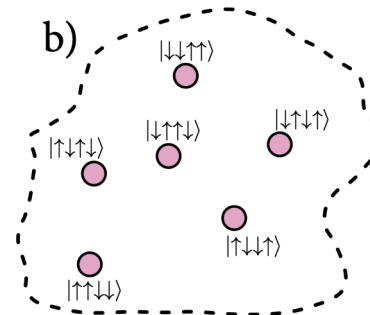
When amplitudes are known the trial ground state energy $\langle \Psi | H | \Psi \rangle$

is a bilinear function of signs s_i , and

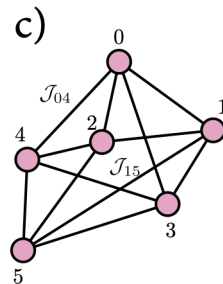
we have Ising optimization problem in K -dimensional space; K is very big but it turns out that the model is not glassy and can be optimized without too serious problems



Real lattice

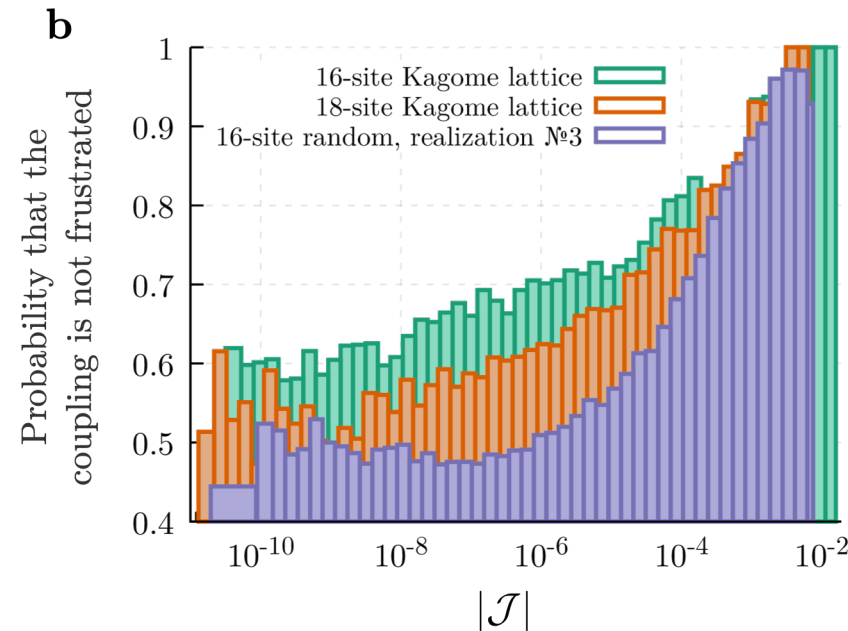
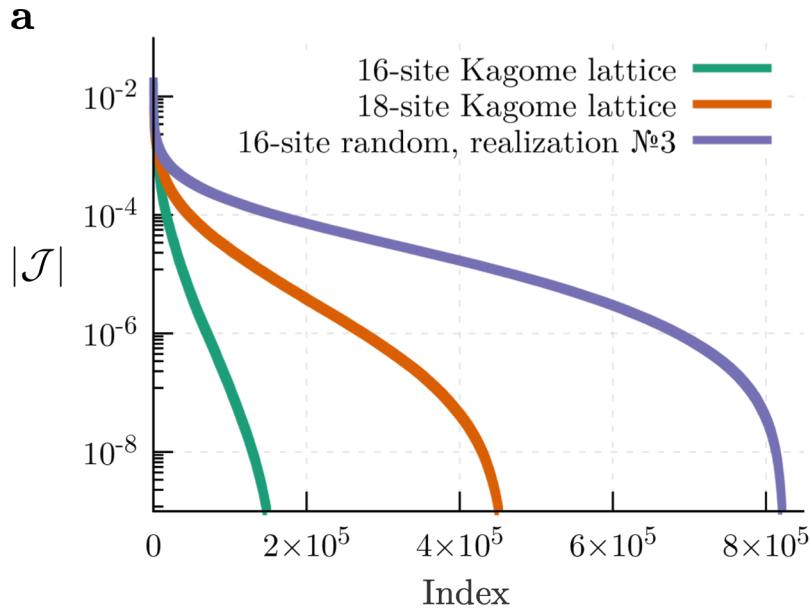


Hilbert space



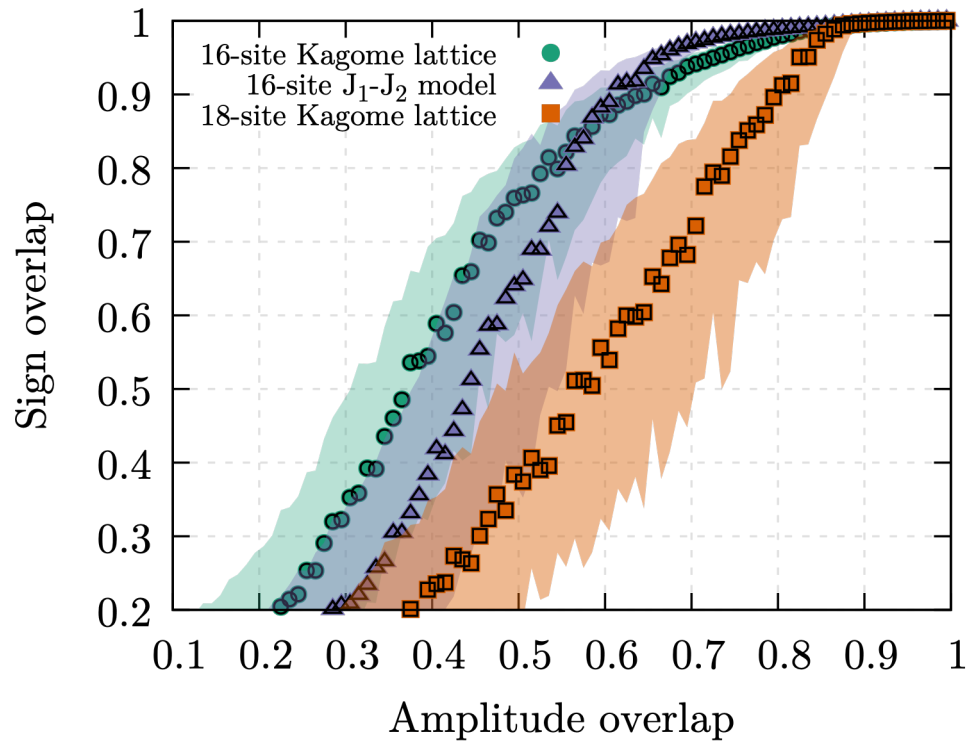
Ising model

Further development II



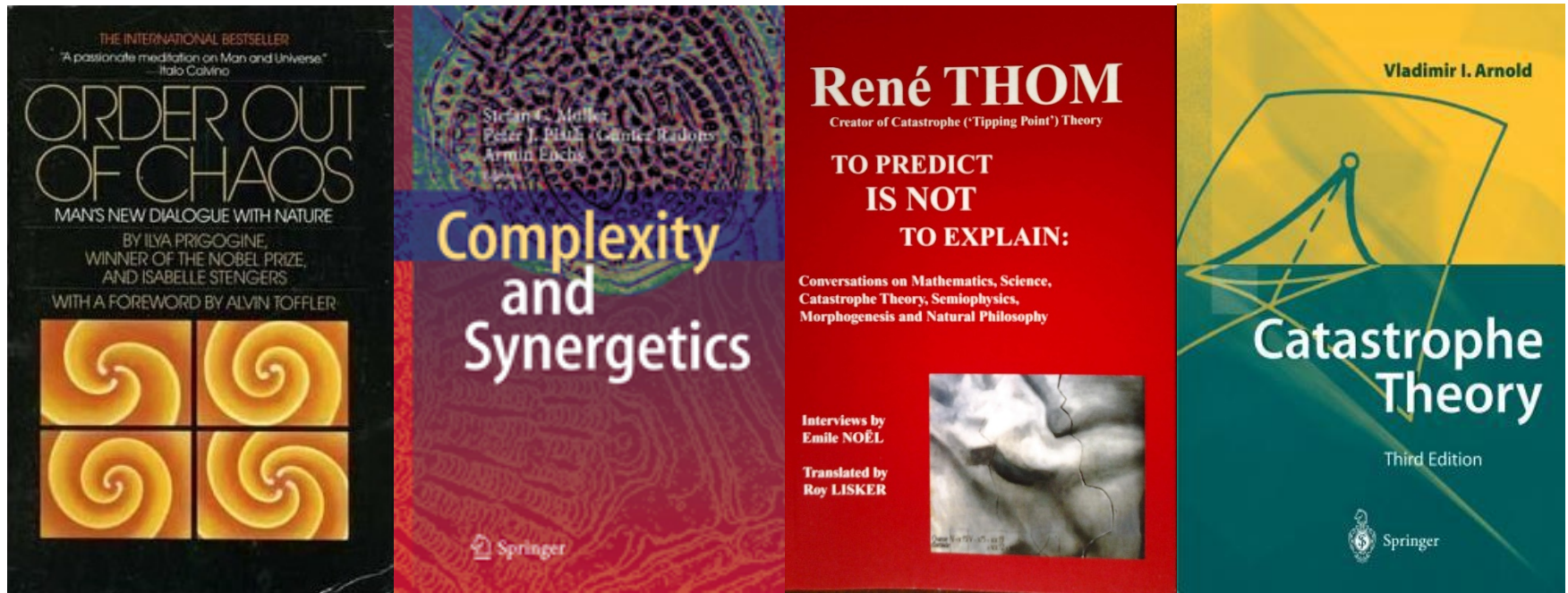
It turns out that even for initially frustrated quantum spin models the effective Ising model is not frustrated, both couplings are small and optimization is quite efficient

Further development III



The quality of optimization is quite robust with respect to uncertainties in amplitudes (overlap with the exact ground state)

To summarize: How it was in 1960th-1980th



People were very enthusiastic on applications of theory of dynamical systems: attractors, bifurcations, catastrophes – useful for sure **but...**



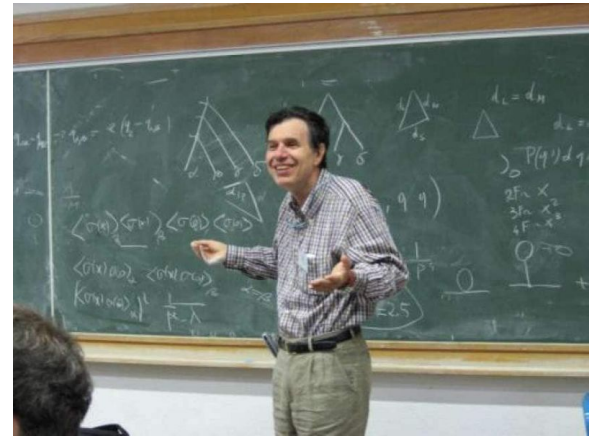
The distance from Benard convection cells to origin of life seems to be too far...

To summarize: Now

Now we try statistical physics approached, our new key words are:
emergence, renormalization group flow, universality classes,
spin glasses, broken replica symmetry, frustrations...

Giorgio Parisi, Nobel Prize in physics 2021

"for the discovery of the interplay of disorder
and fluctuations in physical systems from atomic
to planetary scales."



Actually, disorder is not needed, frustrations are enough
(self-induced spin glass state in Nd)

Whether you can observe a thing or not
depends on the theory which you use.
It is theory which decides what can be observed
(A. Einstein)